Fuel Processing Technology 284 (2026) 108426

Contents lists available at ScienceDirect

Fuel Processing Technology

journal homepage: www.elsevier.com/locate/fuproc

Enhancement of compression ignition engine performance using waste plastic-derived fuel blended with nanoparticles: An experimental and regression analysis

Upendra Rajak [a], Manoj Panchal [a], Abhishek Dasore [b], Norhashila Hashim [c], Ramesh Chandra Mohanty [d], Nimay Chandra Giri [e,*], Soumya Ranjan Das [f,*]

[a] Department of Mechanical Engineering, RGM College of Engineering and Technology, Nandyal 518501, Andhra Pradesh, India
[b] School of Computer Science and Artificial Intelligence, SR University, Warangal, Telangana 506371, India
[c] Department of Biological and Agricultural Engineering, Faculty of Engineering, Universiti Putra Malaysia, Serdang 43400, Selangor, Malaysia
[d] Department of Mechanical Engineering, Centurion University of Technology and Management, Jatni 752050, Odisha, India
[e] Department of Electronics and Communication Engineering, Centurion University of Technology and Management, Jatni 752050, Odisha, India
[f] Manipal Institute of Technology, Manipal Academy of Higher Education, Manipal, India

ARTICLE INFO

Keywords:
Diesel engine
Waste plastics oil
Aluminum oxide nanoparticles
General regression neural network
Performance
Emissions

ABSTRACT

The study is experimental research on the performance, combustion, and emission characteristics of a compression ignition (CI) engine run with waste plastic oil (WPO)-diesel blends supplemented with aluminum oxide (Al_2O_3) nanoparticles. The tested fuel consisted of neat diesel (D100) and WPO-diesel blends (DWPO10, DWPO20, DWPO30, and DWPO40). Furthermore, 25, 50, and 100 ppm of Al_2O_3nanoparticles were suspended in DWPO20. The results indicate that of all the fuels that have been tested, DWPO20 25 ppm Al_2O_3had the brake thermal efficiency (BTE) (32.36%), which was higher than DWPO20 without nanoparticles (31.68%), while also reducing the brake specific fuel consumption (BSFC). When the WPO proportion was raised, the peak cylinder pressure did decrease slightly, but DWPO20 maintained the same combustion behavior as D100. The emission levels of nitrogen oxides (NO_x) were also increased with the growing CR, but the levels of CO and HC were reduced with the inclusion of the nanoparticles because of improved oxidation kinetics. Artificial neural network (ANN) and general regression neural network (GRNN) models were developed to predict engine performance and emissions. The models reported excellent predictive performance (R^2=0.85–0.96) and they were able to reproduce physically consistent trends of combustion and emission with varying operating conditions.

1. Introduction

Compression ignition (CI) engines are widely employed in transportation and industry due to their dependability and low cost. As renewable energy sources have developed, petroleum as a primary fuel has become less dominant worldwide [1]. For CI engines, renewable energy sources as first-, second-, third-, and fourth-generation fuels have been examined. They may be able to substitute petroleum-based fuel for CI engines with renewable energy sources to reduce harmful emissions [2]. Harmful emissions from internal combustion engines represent a major global environmental challenge. Therefore, the scientists and engineers are seeking alternative production control mechanisms besides traditional devices for treating exhaust gas, such as the diesel particulate filter and catalytic converter. One emerging approach is the use of fuel-borne nanoadditives to fulfill the growing energy requirement [3].

Several studies have investigated the impact of WPO blended with diesel (D100) at 20% (DWPO20), 40% (DWPO60), 50% (DWPO50), and 100% (WPO100) and CeO_2 (50 ppm) at different engine loads with CR17.5. They found that the drop in hydrocarbon (HC) and carbon monoxide (CO) emissions for DWPO20 + 50 ppm CeO_2 [4]. The addition of nanoparticles to WPO and D100 is an effective measure to improve burning, which reduces exhaust emissions, including NO_x, carbon monoxide (CO), and carbon dioxide (CO_2) [5]. The author examined the

* Corresponding authors.
E-mail addresses: upendrarajak@rgmcet.edu.in (U. Rajak), manojpanchal@rgmcet.edu.in (M. Panchal), dasore.abhishek@sru.edu.in (A. Dasore), norhashila@upm.edu.my (N. Hashim), rcmohanty@cutm.ac.in (R.C. Mohanty), nimay.giri@cutm.ac.in, girinimay1@gmail.com (N.C. Giri), soumya.das@manipal.edu (S.R. Das).

https://doi.org/10.1016/j.fuproc.2026.108426
Received 24 December 2025; Received in revised form 21 February 2026; Accepted 23 February 2026
Available online 26 February 2026

impact of magnesium oxide (50, 100, and 150 ppm) with an 80% diesel and 20% biodiesel blend on the DE. It is investigated that the addition of nanoparticles decreases emissions of HC by 17.3% and CO by 14.28%, while increasing NO_x by 5.08% [6]. The influence of WPO blends on a CI DE at different operating conditions. Combinations of DWPO10, DWPO20, DWPO30, H_2 + DWPO10, H_2 + DWPO20, and H_2 + WPO100 are studied on varying loads and fuel injection timings. DWPO10 exhibits a 15.1% improvement in BTE, along with an 11.5% reduction in BSFC. This indicates a decrease in emissions of CO, HC, and smoke [7].

The authors investigated the iron oxide nanoparticles (Fe_3O_4), and waste cooking oil was added to D100 to lower exhaust gas emissions from DE fuel. The experiments were conducted using a CI engine that was continuously operating at 1500 rpm under a range of load conditions. They found that the WCB Fe_3O_4 (75 ppm) combination offers a little higher BTE and a lower BSFC when compared to other blends [8]. The effect of the WPO-D100 blends with rubber seed oil on engine performance was evaluated. Adding biodiesel from rubber seed to WPO and D100 releases as DWPO10, DWPO20, DWPO30, and WPO40 mixtures, they found the performance of the engine was the same as that of diesel, DWPO10, and DWPO20 fuel samples, and the CO emission was lower than with pure diesel [9]. Murugesan et al. [10] examined biodiesel fuel blends with 10, 20, and 30 ppm carbon nanotubes (CNT) added to DWPO20. They identified significant opportunities to reduce HC and CO exhaust emissions without compromising functionality. Nanoparticles in fuel can improve combustion efficiency, although their effect on NO_x emissions remains dependent on operating conditions and dosage. The author evaluated the effects of adding 50, 100, and 150 ppm TiO_2 nanoparticles to nanoparticles blended with WPO. This blend was then tested at 210, 230, and 250 bar injection pressures. Sundar et al. [11] found that the WPO with titanium dioxide might replace D100 at 1500 rpm engine speed, especially at 230 bars injection pressure. According to one study, when 44 ppm of alumina nanoparticles are included in blended fuel, the performance of the engine is enhanced and the emissions are lowered [12]. Another study examined the impact of 20, 50, 60, and 80% of WPO with D100 and graphene oxide (GO) (60 ppm) at different loads and at CR17.5. They showed that the emission of exhaust pollutants such as smoke, HC, and CO emissions had been reduced [13]. Collectively, these studies indicate the potential of nanoadditives to enhance combustion in WPO-diesel systems, but their results are very specific to the case and engine parameters, type of nanoparticle, and dosage. A comparative summary of nanoadditives stated in prior CI engine studies in presented in Table 1 for clear understanding.

A range of nanoparticles such as CeO_2, Fe_3O_4, TiO_2 CNT, and GO, have been explored as fuel additives. In the present work, Al_2O_3 nanoparticles were selected due to several physicochemical and practical considerations. It possesses high thermal conductivity, which supports faster heat transfer and enhanced fuel evaporation, thereby improving combustion efficiency. Its oxygen-rich surface characteristics and catalytic oxidation activity promote more complete combustion, helping to reduce CO and HC emissions. Al_2O_3 is better for large scale use than CeO_2 and TiO_2, due to being more chemically stable and less expensive. In contrast to CNTs and GO, Al_2O_3 is less prone to agglomeration and shows greater resistance to thermal degradation under engine operating conditions. These attributes make Al_2O_3 an applied and effective additive for improving the burning behavior of WPO-D100 blends.

Although nanoparticle aided combustion has been widely researched, the trends of reported emissions particularly of NO_x, HC, CO and the PM, are not always consistent. Some researchers have noticed a lessening of the emissions, attributing them to enhanced oxidation and better mixing of fuel and air. Some others have, however, recorded higher levels of NO_x which are commonly linked to high temperatures of combustion and higher rates of premixed combustion. Such variations in the results could probably be due to differences in the properties of nanoparticles, dose, stability of dispersion, composition of the base fuel, engine loads, timing of injection, and CR. Therefore, a systematic analysis in various operating conditions is required to gain a better insight into how nanoparticles affect emissions in a WPO-diesel combustion engine.

Table 1
Comparative analysis of nanoparticles as presented in the literature.

Nanoadditives	Condition	Results	References
CeO_2 nanoadditives	DWPO20 with 25, 50, and 100 ppm at a single cylinder diesel engine.	BTE is higher by 6% and there is a reduction in CO by 30% and HC by 6.2%.	[4]
Fe_3O_4 nanoadditives	Biodiesel from waste cooking oil with 50, 75, and 100 ppm of Fe_3O_4.	BTE is higher and there is a reduction in fuel consumption with WCB FeO75.	[8]
carbon nanotubes (CNT) nanoadditives	DWPO20 with 20 ppm (CNT) single cylinder diesel engine.	BTE is higher and there is a reduction in smoke by 11.9%, CO by 21.8%, and HC by 22.7% with DWPO20 with 20 ppm CNT.	[10]
TiO_2 nanoadditives	WPO with TiO_2 at different speeds and injection pressures.	BTE is higher by 2.5%, and there is a reduction in smoke but a higher NO_x emission by 36% with the addition of TiO_2 nanoadditives.	[11]
Al_2O_3 nanoadditives	*Azolla pinnata* biodiesel (30%)-diesel blend at 25, 50, and 75 ppm Al_2O_3.	BTE and NO are higher and there is a reduction in smoke, HC, and CO with the addition of Al_2O_3 (44 ppm).	[12]
Graphene oxide (GO)	WPO20 with 60 ppm GO nanoparticles.	BTE is higher by 7.8% and there is a reduction in SBFC by 22.7% with GO nanoparticles.	[13]
Al_2O_3 and TiO_2 nanoadditives	*Guizotia abyssinica* (L.) oil (20%) with diesel at 100 ppm of Al_2O_3 and TiO_2	BTE and NO_x are higher and there is a reduction in CO with the addition of Al_2O_3 (100 ppm).	[26]
Multiwalled carbon nanotubes (N-MWCNTs) nanoadditives	Jojoba biodiesel (20% and 30%) was blended with 10% as known as JDE1 and JDE2.	BTE by 8% and NO_x by 3% are higher and there is a reduction in soot by 25%, HC by 16%, and CO by 37%, BSFC by 5% with the addition of Al_2O_3 (44 ppm).	[29]

While earlier works have explored WPO combustion and the usage of nanoparticle additives in fuel, several important gaps persist. Many studies have been limited to a single CR and a narrow range of blend proportions or one nanoparticle concentration, which restricts the broader applicability of their inferences. In particular, the collective influence of WPO-D100 blends with Al_2O_3 nanoparticles across a wide range of CR has not been examined in adequate detail. Moreover, most previous studies rely primarily on experimental trend analysis, with relatively little use of AI-based models to forecast performance and extend the applicability of the outcomes. The physical consistency of AI-based predictions with combustion and emission mechanisms has also not been rigorously validated. Most previous studies investigating the effects of compression ratio, fuel blend proportion, and nanoadditives rely on conventional experimental or design of experiments (DOE) approaches. While DOE methods are suitable for localized parametric analysis, they become inefficient when multiple interacting variables exhibit strong nonlinear behavior, as is typical in WPO-diesel combustion systems enhanced with nanoparticles. Moreover, DOE-based studies are generally restricted to discrete operating points and provide limited predictive capability beyond the tested conditions. In contrast, data-

driven techniques such as Artificial Neural Networks (ANN) and General Regression Neural Networks (GRNN) offer practical complement. These models can learn relationships between operating parameters of engine and their responses specifically performance and emission responses, allowing rapid prediction within the trained range, enhanced interpretation of parameter interactions, and lowered dependence on extensive experimental trials. As a result, AI-based modelling offers a structured and computationally efficient way to explore how CR, fuel blend composition, and nanoparticle dosage interact and affect engine behavior.

The present work is novel in that it combines multi-CR engine testing (15:1–18:1) with ANN- and GRNN- based modelling for Al_2O_3-enhanced WPO-diesel blends. To the best of the authors' knowledge, no existing literature has systematically coupled compression ratio variation with dual AI regression frameworks, enabling both mechanistic experimental evaluation and generalized predictive optimization of engine performance and emissions. This combined experimental-AI framework provides a robust pathway for scalable optimization of alternative fuel combustion in CI engines.

2. Experiments and materials

2.1. Properties of fuel

The non-catalytic process of thermal pyrolysis of mixed post-consumer plastic waste, predominantly polyethylene (PE) and polypropylene (PP) was used to obtain WPO. Polyvinyl chloride (PVC), metals, and dirt materials were pre-treated by manual segregation and washing. Clean plastic waste was subsequently dried and shredded mechanically in order to have even particle sizes, which were then fed into the reactor [14,15]. Pyrolysis was done in a closed system with no oxygen and in a fixed-bed reactor at a temperature between 300 °C and 500 °C. To avoid oxidation by thermal decomposition, an inert atmosphere was used. In such circumstances, plastic feedstock was shredded into hydrocarbon vapours and channeled to a condensation unit. Condensed liquid fraction was pooled as WPO, whereas non-condensable gasses were harmlessly vented [16], as shown in Fig. 1 (a). The oil collected was left to settle and filtered to get rid of residual char. Lastly, it was placed under airtight conditions and stored at ambient conditions before being blended with fuel and later characterized. The produced WPO exhibited high calorific value, negligible sulphur content, low moisture presence, and near-neutral pH, making it suitable for CI engine applications [17,18].

On a volumetric basis, WPO was combined with D100 to make four fuel blends as highlighted in Fig. 1 (b): DWPO10 (10% WPO + 90% diesel), DWPO20 (20% WPO + 80% diesel), DWPO30 (30% WPO + 70% diesel), and DWPO40 (40% WPO + 60% diesel). Mixing was done in the controlled laboratory conditions to produce homogeneous mixing. All the blends were then magnetically stirred for 30 min, after which all blends were ultrasonicated for 45 min to increase homogeneity and eliminate phase separation. For nanoparticle-enhanced fuels, Al_2O_3 nanoparticles were introduced into the DWPO20 blend at concentrations of 25, 50, and 100 ppm. The mixtures were magnetically stirred and then ultrasonicated to lessen particle agglomeration and ensure uniform dispersion throughout the fuel. The stability of the WPO-D100 blends and the nanoparticle-enhanced blends was assessed through visual sedimentation observations over 72 h, along with UV–Vis spectroscopy, zeta potential measurements, and centrifugation tests. No visible sedimentation or phase separation was noticed during the test period, indicating adequate dispersion stability under the experimental conditions. The physicochemical properties of neat diesel (D100), WPO, and the prepared blends are summarized in Table 2.

2.2. Characterization of Al_2O_3 nanoparticles

The morphology, surface structure, and elemental composition of Al_2O_3 nanoparticles utilized in the current study have been examined

Table 2
Properties of testing a fuel sample with a standard.

Property	D100	WPO	DWPO20	ASTM Method
Calorific value (MJ/kg)	45.5	39.8–44.3	40.37	D240
Cetane number	48	49.3	53.2	D4737
Density (kg/m^3) at 15 °C	838	850	840.48	D4052
Flash point (°C)	53	42	50.72	D93
Viscosity (mm^2/s) at 40 °C	3.0	3.4	3.07	D445

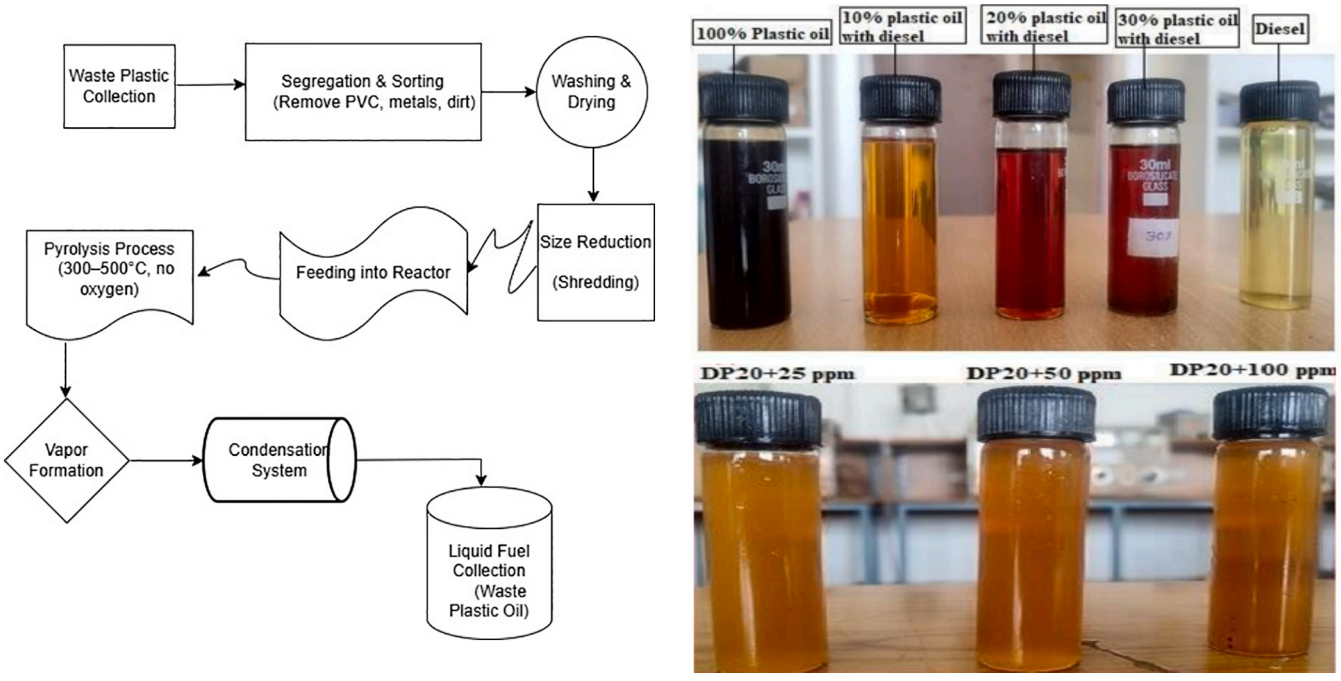

Fig. 1. (a). WPO production from waste plastics. (b). WPO-D100 with Al_2O_3 blended fuel sample.

using scanning electron microscopy (SEM) and energy dispersive X-ray spectroscopy (EDX). SEM images (Fig. 2a) indicate that the morphology of the nanoparticles is almost spherical with observable agglomeration that is characteristic of metal oxide nanoparticles because they have high surface energy. The estimation of particle size quantitatively was performed by analysing SEM micrographs with image-processing software. The main particle size was found to be concentrated in the nanometre range, with secondary agglomerates being in cluster form with sizes reaching to the submicron scale. This agglomeration would occur under dry conditions and is usually reported in the case of Al_2O_3 nanoparticles that find applications in combustion and fuel additives.

The analysis findings of the EDX test (Fig. 2b) confirm the presence of aluminum and oxygen as the main elements with the weight percentages of 24.6% Al and 75.4% O that indicate high purity of materials and the absence of serious contaminants (Table 3). The even distributions of elements facilitate a homogenous catalytic and thermal behavior during combustion. In reference to combustion, the moderate agglomeration does not create any issue for the efficacy of nanoparticles, but agglomerates tend to partially decompose and redisperse under high in-cylinder temperatures. The presence of nanoscale clusters enhances heat transfer, oxidation, and reaction kinetics; therefore, it influences the efficiency of combustion and emission characteristics as observed in this study. The summary of the elemental composition of the sample, as per the findings of EDX analysis summarized in Table 3, indicates that the primary elements are of aluminum and oxygen, which are in line with the Al_2O_3 nanoparticles. Fig. 2(a) presents the SEM micrograph of Al_2O_3 nanoparticles; it presents agglomerated nanoscale clusters, which are porous in nature. The element composition of Al_2O_3 is confirmed in Fig. 2(b), as the strongest peaks are Al Kα and O Kα.

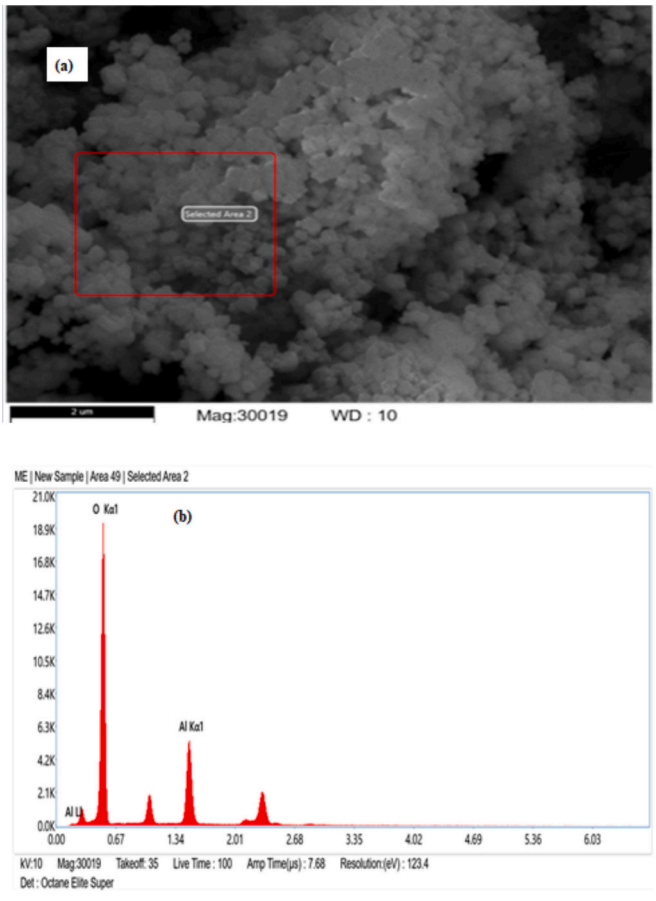

Fig. 2. (a) SEM image and (b) EDX analysis for Al_2O_3.

Table 3
Percentage composition of the elements.

Element	Weight %	Atomic %	Net Int.	R	A	F
O K	75.4	83.8	1015.0	0.9325	0.6590	1.0000
Al K	24.6	16.2	382.9	0.9526	0.8147	1.0019

2.3. Experimentation

To confirm the outcomes, tests were done on a 4-stroke, single-cylinder, direct- injection DE that makes 3.5 kW at 1500 rpm. Table 4 shows the technical specifications, and Fig. 3 shows a diagram of the test engine arrangement. A dynamometer is associated with the engine and applies a load. By a normal injection process, the test trials were injected straight into the ignition chamber at a constant temperature and fuel injection pressure. A solenoid-controlled electronic burette associated with the engines fuel tank and fuel pump measured fuel consumption. A differential pressure sensor in the air box measured air usage. A surge tank kept the air flowing into the intake manifold at a steady rate and also cut down on engine atmospheres. A charge amplifier was coupled to a piezoelectric pressure transducer (Kistler) that was put in the cylinder head to measure the gas pressures inside the chamber. Using the recorded in-cylinder pressure and 1-D thermodynamic models, we figured out the heat release rates. The parameters listed in Table 4 represent the fixed engine specifications and baseline operating conditions maintained during the experimental investigations.

2.4. Uncertainty analysis

To ensure the reliability and repeatability of data, all engine tests were performed at steady-state operating circumstances. Before commencing data collection, the engine was left to stabilize for 10–15 min at every test condition until the main parameters, such as engine speed, EGT, fuel rate, and emission concentrations, showed that their values did not fluctuate significantly. The experimental tests were then repeated three times under the same operating conditions (constant speed, constant load, injection timing, and injection pressure), and further analysis of the mean values was taken to eliminate random experimental errors as much as possible. All measurement instruments and emission analysers were calibrated before experimentation according to manufacturer guidelines. Gas analysers for CO, HC, and NO_x were calibrated using zero and span calibration gases, while the smoke meter was calibrated using standard reference filters. Sensors for speed, load, pressure, and temperature were calibrated against standard reference instruments to ensure accuracy. Measurement uncertainty was evaluated using the error propagation method, as reported in the literature [19,20]. In the present study, measurement uncertainties arise from multiple independent sources, including sensors, analysers, and derived performance parameters. The uncertainty associated with each measured or calculated quantity was assumed to be statistically independent.

Thus, the general experimental uncertainty was determined by the root-sum-square (RSS) approach, which is commonly used for uncertainty spread in engine testing. Using this method, there is a cumulative

Table 4
Technical specifications and operating settings of the test engine.

Make	Kirloskar
Model	TV1
Bore x stroke	87.5 mm × 110 mm
Swept volume	661.45 (cc)
Connecting rod length	234.00 (mm)
Compression ratios	15:1 to 18:1
Rate speed	1500 rpm
Cooling method	water
Injection timing	23° b TDC

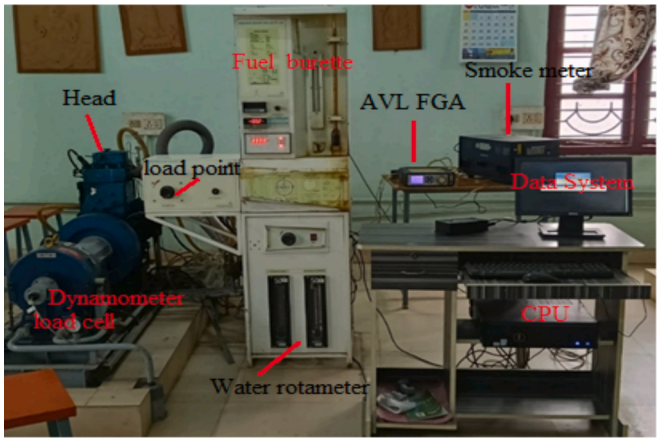

Fig. 3. Experiment test ring.

impact of individual uncertainties on the final reported outcomes. As such, the overall uncertainty (U_n) was computed by the RSS formulation as in eq. (1), where $\frac{\partial x_i}{x_i}$ is the ratio of the uncertainty of the individual measured or derived quantity. According to the individual instrument uncertainties listed in Table 5, the total experimental uncertainty was considered±3.03%, which is within the acceptable limits for engine performance and emission investigations. The low uncertainty value indicates the repeatability and reliability of the experimental measurements.

$$U_n = \sqrt{\left(\frac{\partial x_1}{x_1}\right)^2 + \left(\frac{\partial x_2}{x_2}\right)^2 + \left(\frac{\partial x_3}{x_3}\right)^2 + \ldots \left(\frac{\partial x_n}{x_n}\right)^2} \quad (1)$$

$$U_n = \sqrt{(0.2)^2 + (0.2)^2 + (0.5)^2 + (1.0)^2 + (0.15)^2 + (1.0)^2 + (0.5)^2 + (0.3)^2 + (0.3)^2 + (1.4)^2 + (2.1)^2} = \pm 3.03\%.$$

2.5. Framework of the study

The framework of the current study is a combination of experimental research and physics-informed AI modelling that can be used to assess the performance and emission profile of a CI engine using Al_2O_3-enhanced WPO-diesel blends. Fig. 4 represents the framework

Table 5
Uncertainty of measuring instruments and derived parameters.

Quantity	Uncertainty (%)
Measured instruments	
Encoder	±0.2
Load cell	±0.2
Pressure sensor	±0.5
Speed sensor	±1.0
Temperature sensor	±0.15
Smoke meter	±1.0
NO_x sensor	±0.5
CO sensor	±0.3
HC sensor	±0.3
Derived parameters	
BTE	±1.4
BSFC	± 2.1

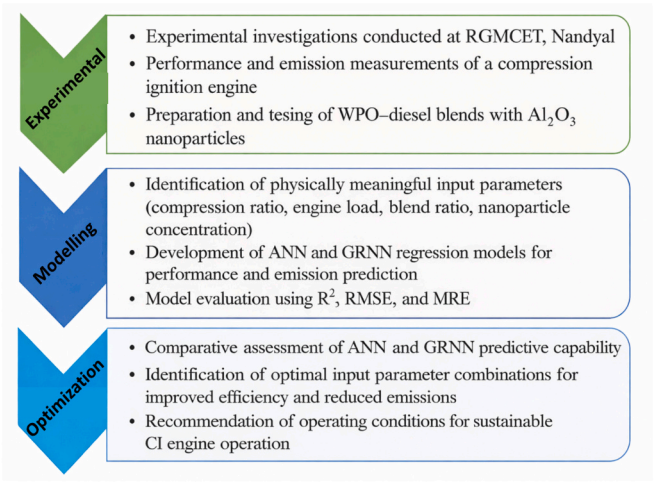

Fig. 4. Framework of the proposed experimental and AI-based modelling approach.

and consists of the sequential process of data acquisition in the experiments, through to AI-based regression and performance optimization. The ANN and the GRNN models were selected with CR, engine load, WPO blend ratio, and Al_2O_3 nanoparticle concentration as the input parameters, which directly impact combustion and emission formation. These factors control the in-cylinder pressure-temperature development, fuel atomization, ID, and oxidation rate. The output parameters, such as BTE, BSFC, and regulated exhaust emissions (NO_x, CO, and HC), are some of the most important macroscopic parameters of engine performance and their effect on the environment. This framework ensures that the developed ANN and GRNN models keep on being physically interpretable rather than only data-driven.

2.6. ANN and GRNN modelling and evaluation

The ANN modelling process is divided into two phases: training and testing. The experimental data was randomly split into 70% to train and 30% to test to ensure strong generalization. The neural network used was a feed-forward back-propagation with one hidden layer. This model structure effectively captures non-linear relationships between engine performance and emission measurements [21]. Training was done by the Levenberg-Marquardt algorithm, which is fast convergent and applicable to regression problems. The hidden layer size was varied in

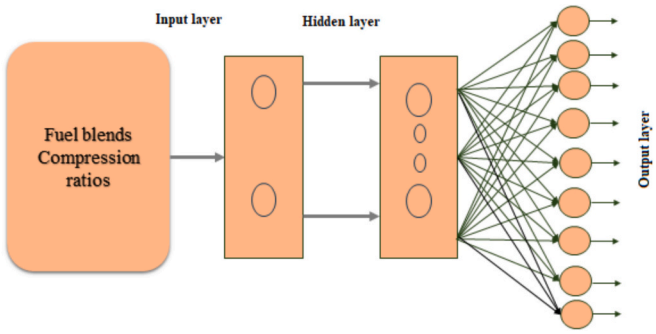

Fig. 5. Architecture of ANN model.

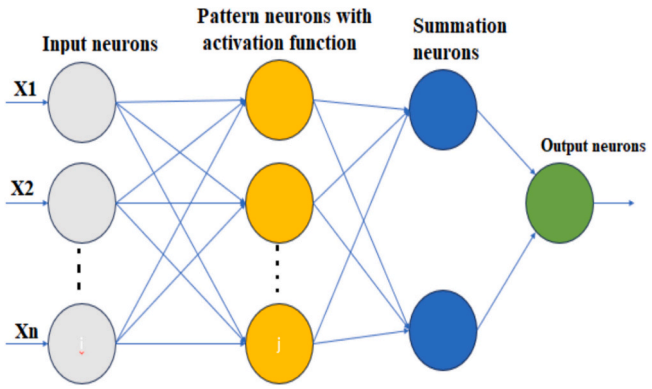

Fig. 6. Architecture of GRNN.

numbers from 1 to 10, and the hyperbolic tangent activation function was chosen, as it has been successfully employed in nonlinear combustion modelling [22,23]. Fig. 5 illustrates the ANN architecture.

In parallel, GRNNs were trained as an alternative regression model. GRNNs are memory-based, probabilistic networks that are highly suitable in case of small experimental data and nonlinear function approximation [24]. GRNNs, unlike the traditional ANN models, do not need an iterative training process, and hence the process can be trained rapidly whilst achieving high accuracy. The GRNN design adopted in this experiment is shown in Fig. 6. The coefficient of determination (R^2), mean relative error (MRE), and root mean square error (RMSE) metrics were used to assess the model performance by using Eqs. (2)–(4) [25,26]. These statistical measures were used to determine the predictive power of ANN and GRNN models of predicting experimentally observed relationships between physically significant input parameters and engine performance and emission outputs.

$$R^2 = 1 - \left\{ \frac{\sum_{i=1}^{n} (E_i - P_i)^2}{\sum_{i=1}^{n} (P)^2} \right\} \tag{2}$$

$$\mathrm{MRE}(\%) = \frac{1}{n} \sum_{i=1}^{n} \left| 100 \frac{(E_i - P_i)}{(P_i)} \right| \tag{3}$$

$$\mathrm{RMSE} = \sqrt{\frac{i}{n} \sum_{i=1}^{n} (E_i - P_i)^2} \tag{4}$$

where the experimental data, predicted value, and number of data values are denoted by E_i, P_i, and n =, respectively.

2.6.1. Prevention of overfitting and model robustness

Model robustness was ensured by controlling network complexity and by evaluating predictive performance on unseen data. The comparable statistical performance obtained for both training and testing datasets, reflected by consistent R^2, MRE, and RMSE values, indicates that the developed models learned the underlying physical trends rather than memorizing experimental noise. The ANN architecture of small size with a single hidden layer also constrained the over-flexibility of the model, thus minimizing the overfitting possibility. In the case of the GRNN model, overfitting was automatically reduced by its non-iterative design and dependence on a smoothing parameter that controls the bias-variance trade-off. The pressing factor was selected to achieve a balance between prediction and noise sensitivity so that there was steady regression behavior. Overall, the consistency of statistical indicators across datasets checks the robustness and reliability of both ANN and GRNN models.

2.6.2. Model applicability and limitations

Although the ANN and GRNN models demonstrated strong predictive capability within the investigated operating range, their applicability is limited to the experimental conditions considered in this study. The models can be applied to WPO-diesel blends that are 10–40% WPO, have 25–100 ppm Al_2O_3 nanoparticles, have CRs of 15:1–18:1 and have a constant engine speed of 1500 rpm. The extrapolation beyond these limits, e.g., increased nanoparticle concentrations, variable engine speeds, variable injection timings, or different engine configurations, might be subject to lower predictive accuracy, so it is not advisable without further experimental validation. The direction of future research can expand the dataset to a wider range of operating conditions, enhancing the generalizability of the model and allowing sophisticated data-driven optimization models.

3. Results and discussions

3.1. ANN model prediction

The ANN architecture establishes the optimal prediction. The ANN prediction is shown in Fig. 7 for different parameters of the engine. The architecture of model consists of two input layer as fuel blend, and CR), hidden layers and nine output parameters (BTE, BSFC, max cylinder pressure, EGT, ID, smoke, CO, HC, and NO_x emissions), as shown in Table 6. Trial and error yields optimal enhanced information capacity and diminishes network size.

3.2. GRNN model prediction

The GRNN architecture establishes the optimal prediction [27]. The GRNN diagram is presented in Fig. 8 (a-f). The architecture of model consists of two input layer as fuel blend, and CR), hidden layers and nine output parameters (BTE, BSFC, max cylinder pressure, EGT, ID, smoke, CO, HC, and NO_x emissions) as shown in Table 7. Trial and error yields optimal enhanced information capacity and diminishes network size. It is noted from Table 6 and Table 7, quantitatively R and MSE are consistent for testing, training and validation data, which indicates a very good generalization and no over fitting of data.

3.3. Brake thermal efficiency

The BTE versus CR (15:1, 16:1, 17:1, and 18:1) for eight different fuel samples at 1500 rpm under full load is presented in Fig. 9. The graph indicates that at higher engine CRs, the use of WPO as fuel results in a slight reduction in BTE compared to pure diesel (D100). At 1500 rpm, the engine achieves a BTE of 32.36% when using a mixed fuel of DWPO20 with 25 ppm Al_2O_3 nanoparticles, while it achieves a BTE of 31.68% when using DWPO20 blend. At full load condition, the BTE values for D100, DWPO10, DWPO20, DWPO30, DWPO40, DWPO20 + 25 ppm, DWPO20 + 50 ppm, and DWPO20 + 100 ppm are 32.38%, 32.19%, 31.68%, 31.41%, 31.68%, 32.4%, 32.08%, and 31.53%, respectively. The statistically substantial increase in BTE of Al_2O_3-included DWPO20 blends is greater than the total experimental error of ±3.03%, so the observed improvement is statistically important and cannot be accredited to measurement variability. Despite their lower calorific value, certain WPO blends display comparable or slightly improved BTE under specific operating conditions, which specifies that thermal efficiency is not governed by fuel energy content alone. At higher compression ratios and full-load operation, combustion-related factors such as improved fuel–air mixing, faster oxidation kinetics, and favourable combustion phasing play a dominant role in determining BTE [28]. Additional benefits of incorporating Al_2O_3 nanoparticles include higher combustion efficiency due to superior ignition properties, catalytic oxidation and higher in-cylinder heat transfer which all offsets the reduced heating value of WPO-based fuels. This is due to the fact that a change in combustion mechanisms is observed to recover and marginally improve BTE at the increased WPO blending ratios (>40%). The greater proportion of aromatic and unsaturated hydrocarbon compounds at higher WPO fractions, can also contribute to the enhanced

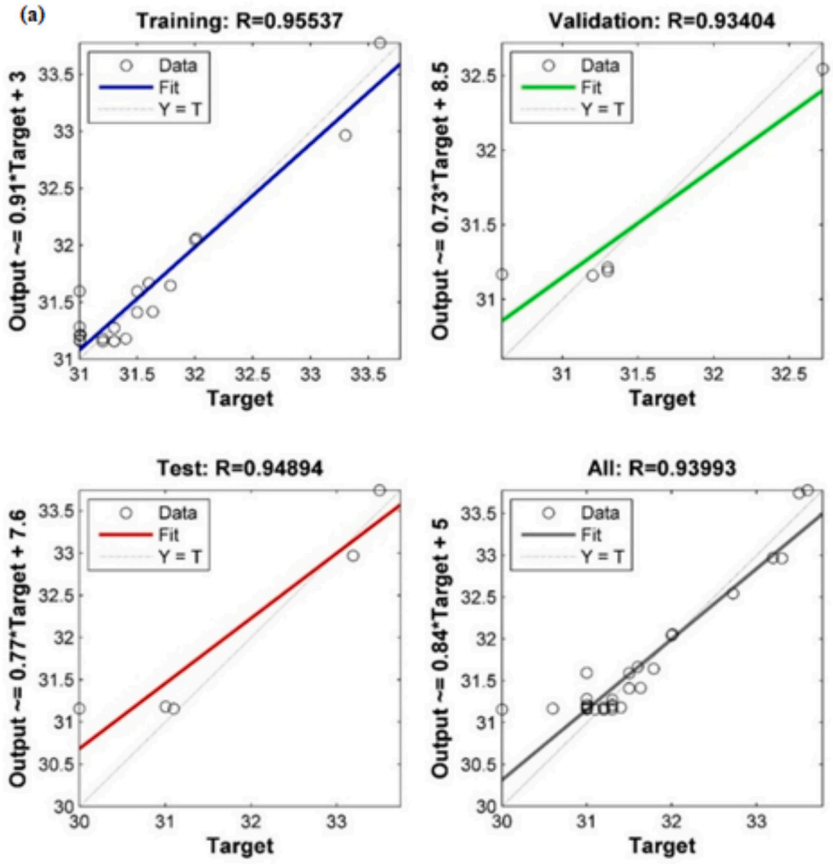

Fig. 7. ANN experimental data vs. predicted data a) BTE, b) BSFC, c) EGT, d) cylinder pressure, e) Ignition delay, f) Smoke emission, g) CO, h) NO_x, and i) HC.

premixed combustion of a mixture during a high-load condition resulting into higher heat WPO, which enhance additional oxidation at higher temperatures, have a role in the realized BTE recovery.

3.4. Brake specific fuel consumption

BSFC versus CR (15:1, 16:1, 17:1, and 18:1) for eight different fuel samples at 1500 rpm under full load is illustrated in Fig. 10. BSFC, influenced by varying fuel combinations, reflects the efficiency with which an engine converts fuel into power; lower BSFC values indicate better fuel economy. The energy content of the WPO blend increases; fuel consumption also increases due to its higher density and lower heat value, which can lead to reduced atomization and imperfect ignition [29–31]. The outcomes indicate that all WPO fuel blends have superior BSFC compared to other fuel blends, with discrepancies starting at 2.62% across all CR levels. Interestingly, when compared to their counterparts without nanoparticles (DWPO20), the Al_2O_3 nanoparticle-enriched blends (DWPO20 + 25 ppm, DWPO20 + 50 ppm, and DWPO20 + 100 ppm) exhibit a notable decrease in BSFC at full load, with decreases of 9.7%, 9.55%, and 9.5%, respectively. These reductions in BSFC are significantly higher than the estimated uncertainty bounds and were consistently observed across repeated trials, indicating statistically reliable fuel economy improvement.

3.5. Exhaust gas temperature

The exhaust gas temperature (EGT) with CR (15:1, 16:1, 17:1, and 18:1) for eight different fuel samples at 1500 rpm under full load is presented in Fig. 11. At this engine speed, the EGT reaches 706 K when using DWPO20 + 25 ppm Al_2O_3 mixed fuel, while it is 686 K for D100. However, when subjected to full load conditions, the EGT values of D100, DWPO10, DWPO20, DWPO30, DWPO40, DWPO20 + 25 ppm, DWPO20 + 50 ppm, and DWPO20 + 100 ppm is 412.8 °C, 457 °C, 430.8 °C, 416 °C, 411 °C, respectively. The nanoparticle blends have a higher EGT than the D100 and WPO fuel blends, as the fuel is better atomized and ignited, leading to a higher HRR in the cylinder. The rise in EGT that is being seen in nanoparticle-enriched blends is beyond the uncertainty of the temperature sensor and indicates a physically consistent rise in heat release in the in-cylinder.

3.6. Cylinder pressure

Fig. 12 (a) for cylinder pressure (P_{max}) and Fig. 12 (b) for HRR with CR (15:1, 16:1, 17:1, and 18:1) for eight different fuel samples tested at 1500 rpm with full load. The cylinder pressure is determined using a piezoelectric pressure sensor, and the amplifier helps to process the signals from the transducer. This pressure specifies the fuel's capacity to create a regular combination with air and to operate successfully. The inspection of fluctuations in cylinder pressure relative to crank angle is crucial in engine analysis, since it delineates the numerous phases of combustion. The $P_{max}$of all fuels increases as CR rises, and the variation trend is the peak cylinder pressure. The results reveal that the P_{max} duration of various oxygenated fuels reduces when compared to DWPO20 + 25 ppm, DWPO20 + 50 ppm, and DWPO20 + 100 ppm. This improvement is due to the increased surface area and improved heat transfer rate, which lead to a better atomization process, heating value, and improved cetane number of the fuel, which increases the P_{max} of the blends when added nanoparticles. The value of P_{max} was found to be 89.9, 87.5, 79.6, 79.0, 76.6, 88.2, 88.3, and 89.9 bar for D100, DWPO10, DWPO20, DWPO30, DWPO40, DWPO20 + 25 ppm, DWPO20 + 50 ppm,

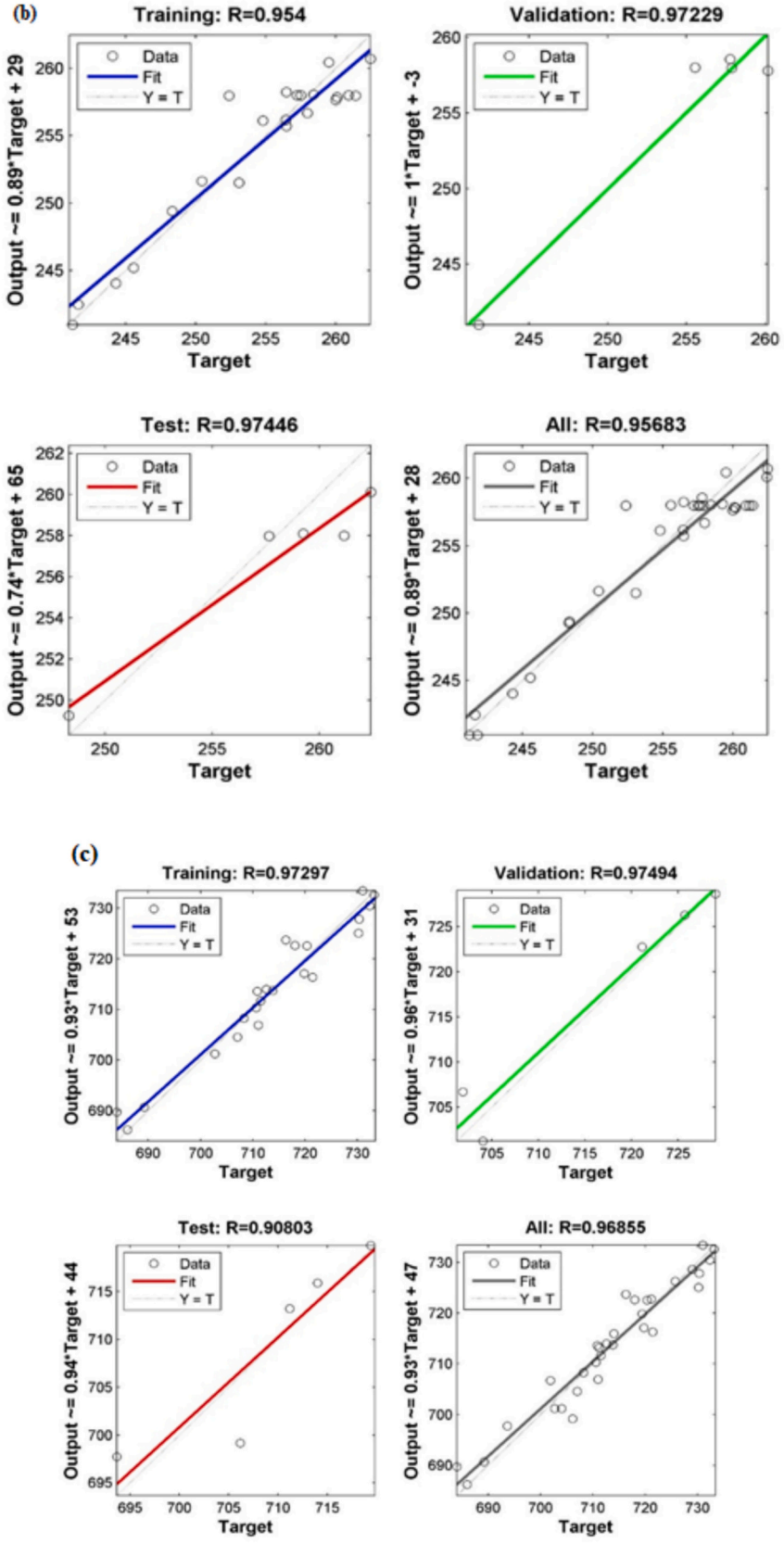

Fig. 7. (*continued*).

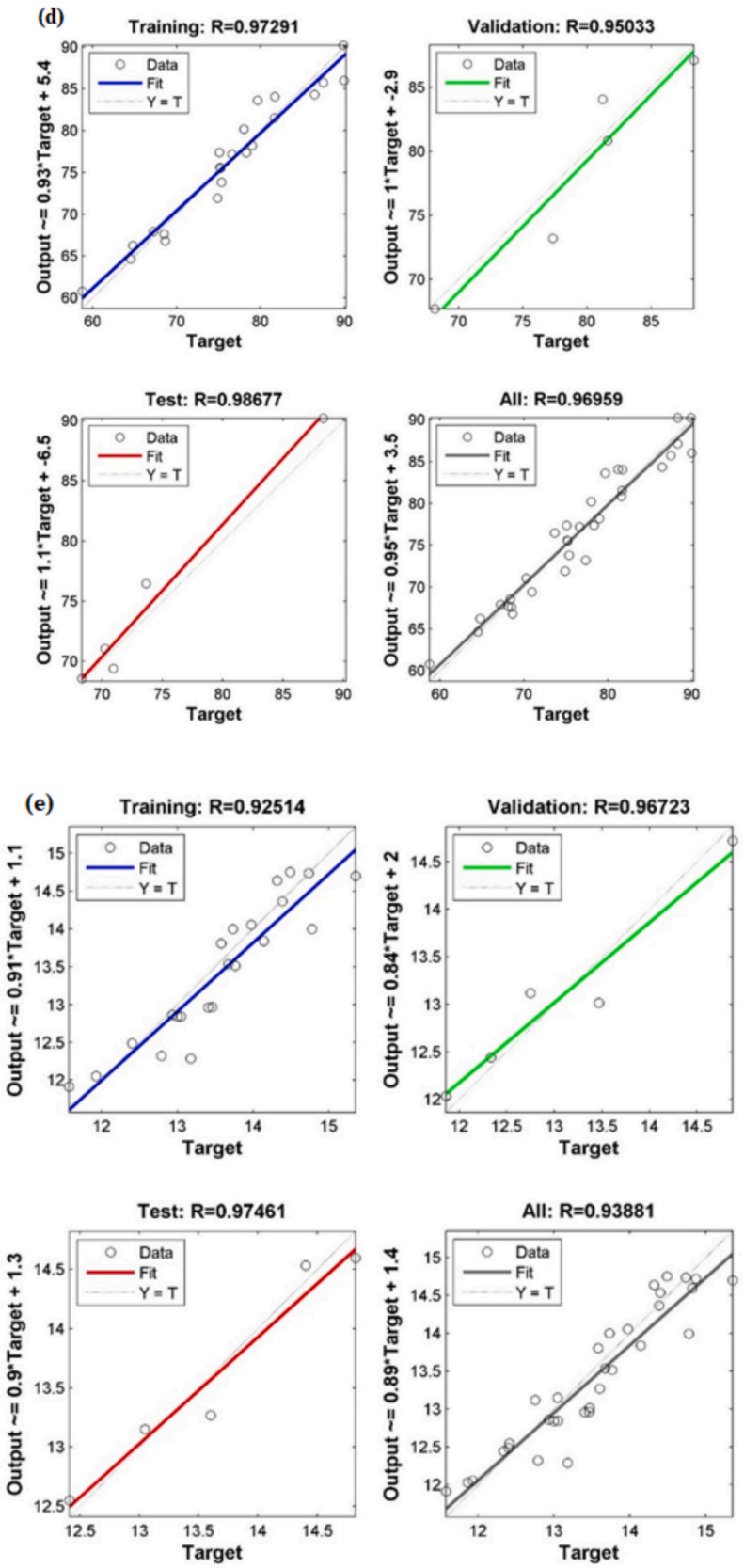

Fig. 7. (*continued*).

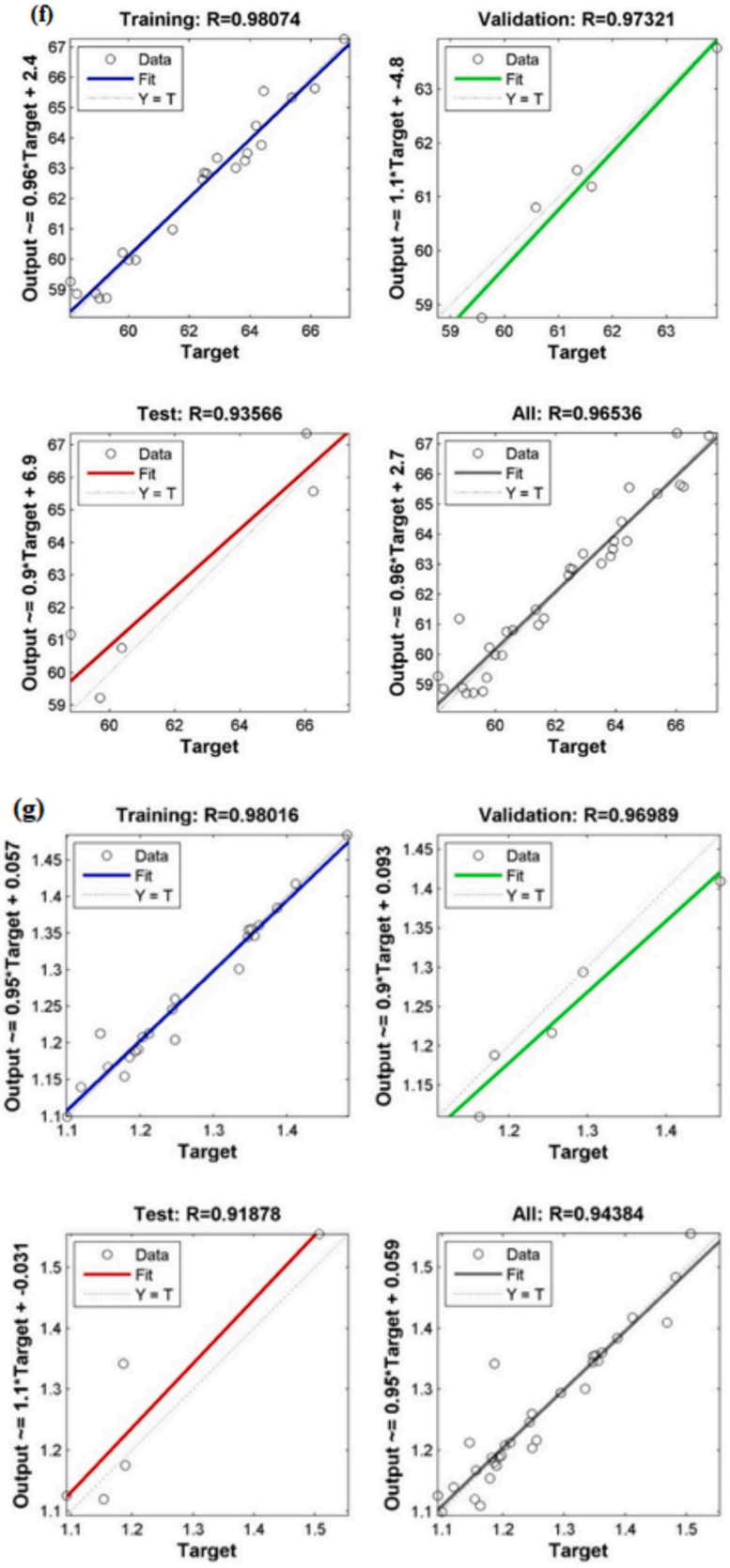

Fig. 7. (*continued*).

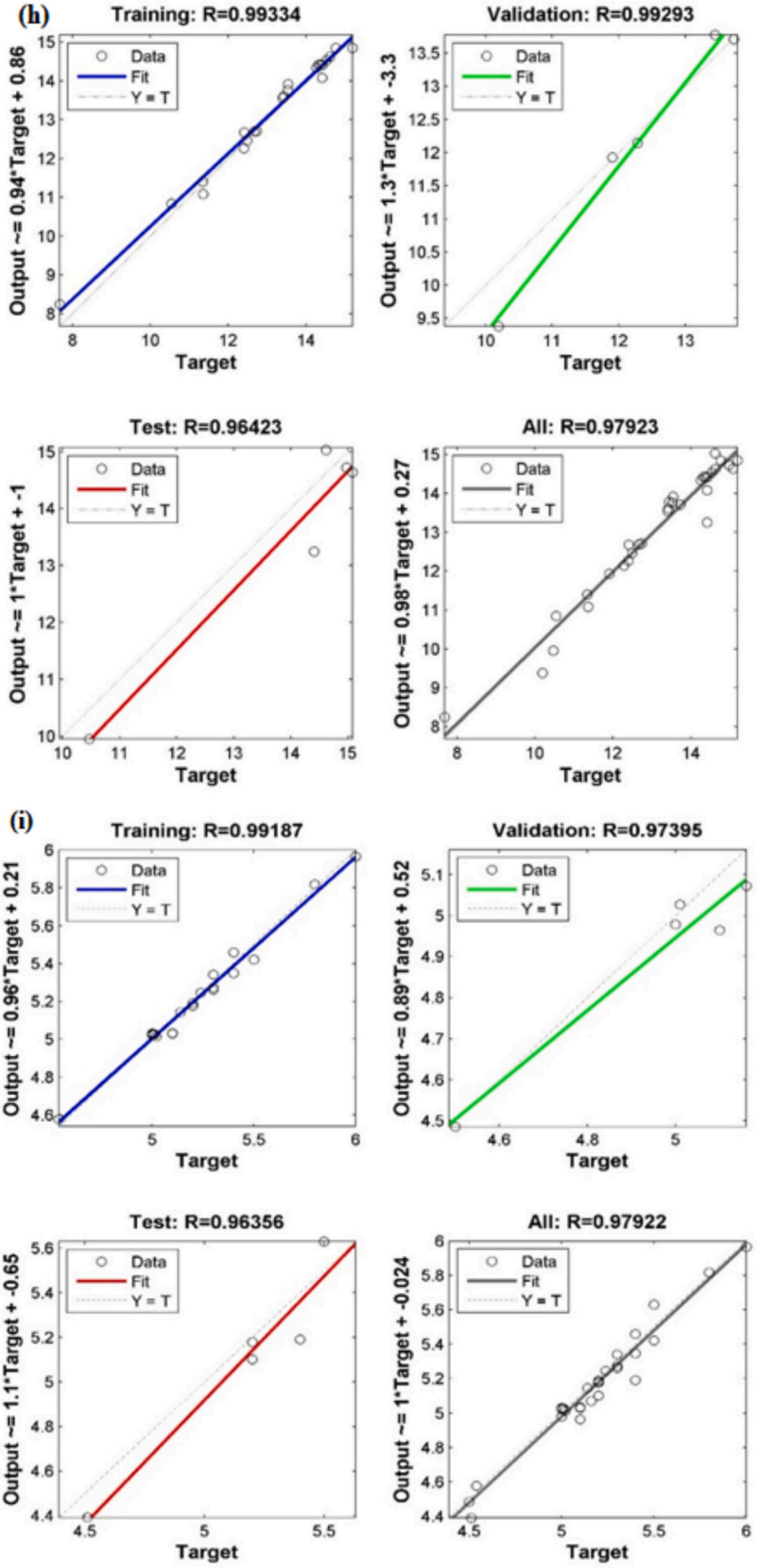

Fig. 7. (*continued*).

Table 6
ANN datasets for training, validation, and testing.

Input Layer	Hidden Layer	Epoch	Metrics	Training sets		Validation sets		Testing sets		All data	
				R	MSE	R	MSE	R	MSE	R	MSE
2	4	16	BSFC	0.954	3.65	0.972	2.57	0.974	3.50	0.956	3.47
2	3	11	BTE	0.955	$4.09*10^{-2}$	0.934	$7.46*10^{-2}$	0.948	$2.97*10^{-1}$	0.939	$8.45*10^{-2}$
2	3	21	EGT	0.972	10.31	0.974	6.86	0.908	14.672	0.968	10.44
2	5	16	Max Pressure	0.972	3.60	0.950	5.52	0.986	2.87	0.969	3.77
2	4	9	Ignition delay	0.925	$1.44*10^{-1}$	0.967	$8.08*10^{-2}$	0.974	$4.18*10^{-2}$	0.938	$1.19*10^{-1}$
2	4	20	Smoke Emission	0.98	$2.57*10^{-1}$	0.973	$1.88*10^{-1}$	0.935	1.65	0.965	$4.56*10^{-1}$
2	8	21	CO	0.98	$4.67*10^{-4}$	0.96	$1.56*10^{-3}$	0.918	$5.18*10^{-3}$	0.943	$1.34*10^{-3}$
2	4	11	NO_x	0.993	$4.86*10^{-2}$	0.992	$1.58*10^{-1}$	0.964	$4.08*10^{-1}$	0.979	$1.19*10^{-1}$
2	5	31	HC	0.99	$1.48*10^{-3}$	0.973	$5.39*10^{-3}$	0.963	$1.69*10^{-2}$	0.979	$4.38*10^{-3}$

and DWPO20 + 100 ppm, respectively, at CR18:1 with full load condition. The differences in peak cylinder pressure among the tested fuels exceed the pressure sensor uncertainty and consistently follow expected thermodynamic trends, confirming the reliability of the measured combustion behavior.

3.7. Ignition delay

Fig. 13 illustrates the ignition delay (ID) in relation to compression ratios (CR) of 15:1, 16:1, 17:1, and 18:1 for eight different fuel samples at 1500 rpm under full load conditions. In a diesel engine (DE), ID refers to the time interval between the initiation of fuel injection and the onset of actual combustion. The ID for all fuel types decreases as the CR increases and the variation trend is the inverse of peak cylinder pressure. The results reveal that the ID duration of various oxygenated fuels reduces when compared to DWPO20 + 25 ppm, DWPO20 + 50 ppm, and DPWO20 + 100 ppm due to increased surface area and improved heat transfer rate, leading to a better atomization process, which decreases the chemical ID of the blends when adding nanoparticles. The reduction in ID with increasing compression ratio and nanoparticle addition is greater than the combined measurement uncertainty and was reproducible across repeated experiments.

3.8. Smoke emissions

The smoke emissions with CR (15:1, 16:1, 17:1, and 18:1) for eight different fuel samples at 1500 rpm with full load are shown in Fig. 14. In internal combustion engines, smoke emissions are a crucial metric for assessing the entire combustion process. Generally speaking, conditions like inadequate atomization, excessive fuel accumulation in the cylinder, and oxygen deficit surrounding the rich blend result in high fuel viscosity. The variation in smoke emissions associated with engine loads is presented in this figure. The figure shows that smoke emissions rise in direct proportion to engine load for both warmed and unheated fuels. When the load of an engine rises, more fuel will be used, and the combustion time and oxygen consumption decrease, and smoke emissions rise. The D100, DWPO10, DWPO20, DWPO30, and DWPO40 have smoke values of 58.9, 62.48, 62.42, 60.2, and 58.2% at rated high load with CR18:1, respectively. Due to inadequate air-fuel mixing and the presence of aromatic ingredients, the pyrolysis oil-mixed fuel exhibited higher smoke emission. When the CR in the engine increased, the smoke emission decreased. Smoke emissions were decreased when Al_2O_3 nanoparticles were added to DWPO20. The combustion process will be enhanced by adding nanoparticles to plastic-based fuels, resulting in reduced smoke generation. The smoke emissions for DWPO20 + 25 ppm, DWPO20 + 50 ppm, and DWPO20 + 100 ppm at 100% load and CR18:1 was found to be 59.03%, 59.27%, and 59.57%, respectively. These are 5.4%, 5.06%, and 4.58% less than the DWPO20. The observed reductions in smoke emissions are substantially larger than the smoke meter uncertainty and therefore represent statistically significant improvements.

3.9. Carbon monoxide emission

The carbon monoxide (CO) emissions with CR (15:1, 16:1, 17:1, and 18:1) for eight different fuel samples at 1500 rpm with full load are shown in Fig. 15. Fuel oxidation was encouraged by varying quantities of AL_2O_3 and DWPO20, which reduce CO emissions. According to these results, compared to D100, using nanoadditives with DWPO20 blends releases less CO. In normal operation, DWPO20 with Al_2O_3 100 ppm emits 7.79% less CO than that of the D100. When an air-fuel mixture burns at a low flame temperature with an insufficient air supply, CO is created during combustion. The majority of the literature review found that using biodiesel instead of D100 generally resulted in fewer CO emissions. It is evident from the figure that higher engine load led to an increase in CO formation. Conversely, with greater loads, partial combustion, brought on by a short combustion time, generates more CO [13]. The reduction in CO emissions with Al_2O_3 nanoparticle addition exceeds the analyzer uncertainty limits, confirming the statistical significance of the observed trend.

As stated above, addition of pyrolysis oil to diesel fuel increases the temperature and pressure in the cylinder to enhance the efficiency of combustion. The findings showed that the mixes of DWPO10, DWPO20, DWPO30, and DWPO40, DWPO20 + 25, DWPO20 + 50, and DWPO20 + 100 ppm had low levels of CO emission as seen in the figure. When the load is full, the CO emissions for D100 (1.193 g/kWh at CR18), the CO emissions for DWPO10, DWPO20, DWPO30, DWPO40, DWPO20 + 25 ppm, DWPO20 + 50 ppm, and DWPO20 + 100 ppm at full load conditions are 1.38, 1.15, 1.19, 1.16, 1.15, 1.16, and 1.1 g/kWh, respectively. The CO emission was also decreased by combining DWPO20 with oxygenated nanoparticles but was higher for the DWPO10 blend. In cases of addition of oxygenated components, the fuel burns completely and results in minimization of CO production. Compared to D100, CO decreased by 3.6%, 2.76% and 7.79% in DWPO20 + 25 ppm, DWPO20 + 50 ppm and DWPO20 + 100 ppm respectively. The fuel with the lowest emissions of any mixed fuel in the current investigation is the DWPO20 + 100 ppm.

3.10. Hydrocarbon emissions

The HC emissions with CR (15:1, 16:1, 17:1, and 18:1) for eight different fuel samples at 1500 rpm with full load are shown in Fig. 16. Incomplete combustion of fuel results in emissions of unburned hydrocarbons. Under specific circumstances, the volatility and viscosity of fuels can impact these emissions and cause them to leak into the exhaust. Because of better charge homogeneity and greater oxygen availability, the study demonstrated that lower loads led to lower levels of HE emissions. Higher loads, however, resulted in higher fuel consumption and HC emissions. The unhealthy hydrocarbons and inadequate combustion create blended fuels that often exhibit higher HC emissions than pure diesel. This data is consistent with earlier blended fuel research. An incomplete fuel-air combination leads to higher HC emissions. The experiment shows that HC emissions rose in tandem with the blend

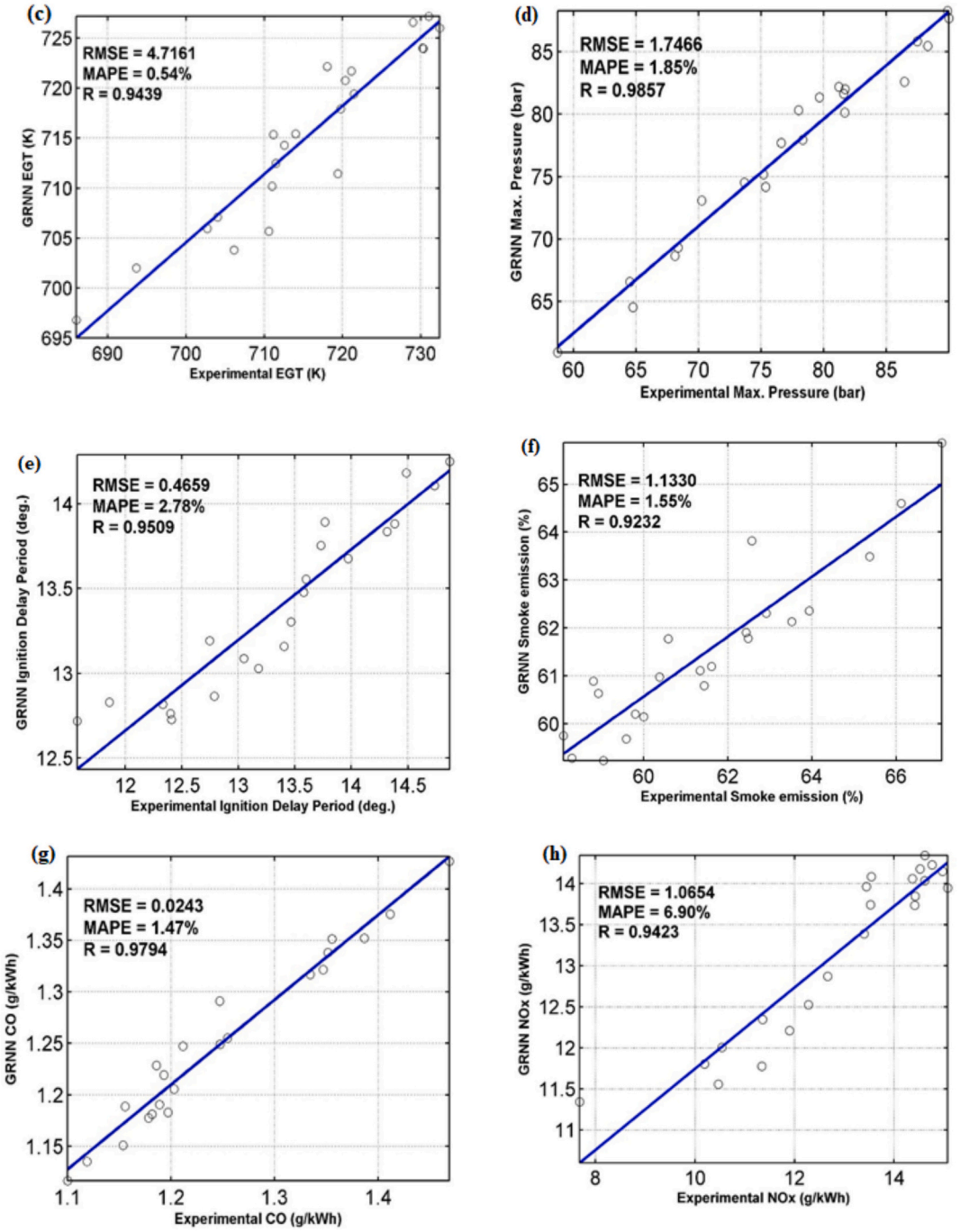

Fig. 8. Comparison of GRNN experimental data versus predicted data: a) BTE, b) BSFC, c) EGT, d) Cylinder pressure, e) Ignition delay, f) Smoke emission, g) CO, h) NO_x, and i) HC.

proportions. The higher mixes of the particles may lead to high HC emissions in a diesel engine. At full load, the conventional engine released HC because of the potent aromatic component in DWPO. On the other hand, under moderate load settings, the addition of DWPO20 with Al_2O_3 100 ppm demonstrated a significant decrease in HC emission, which peaks under higher load levels. When compared to diesel in normal mode, Al_2O_3 at 25, 50, and 100 ppm with DWPO20 decreased HC emissions by 1.85%, 1.85%, and 2.96%, respectively. The DWPO20 + 100 ppm fuel sample was observed to have the lowest HC emission at the CR15:1. Although the reduction in HC emissions is moderate, the observed changes remain outside the experimental uncertainty range and are consistent across repeated measurements.

3.11. NO_x emission

The maximum temperature of the gases inside the combustion chamber, as well as the reaction time available, has a significant impact on NO emission generation. When nitrogen (N_2) from the air reacts with oxygen (O_2) at high temperatures, they are NO_x are created. The three main restrictions that impact the development NO_x of levels in DEs are the adiabatic flame temperature, response time, O_2, the thermal mechanism, the prompt mechanism, and the fuel mechanism. The reflection

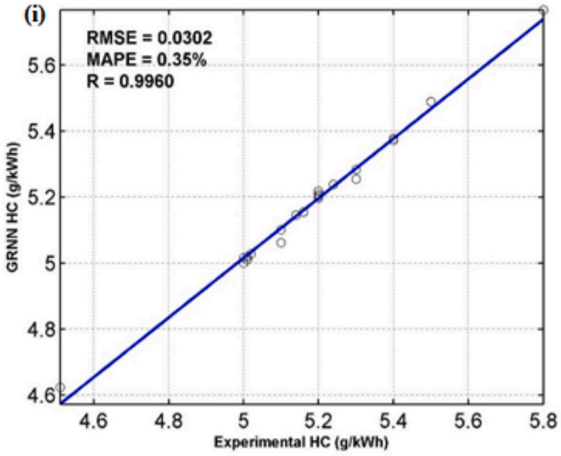

Fig. 8. (*continued*).

Table 7
The correlation parameter between the predicted and measured values.

S. NO.	Parameter	Equation (Training)	Test R-Value	Validation R-Value	RMSE-Test	MAPE-Test
1	BSFC	$Y_{BSFC} = 0.8347\times + 42.2144$	0.9896	0.9943	5.0068	1.47%
2	BTE	$Y_{BTE} = 0.7713\times + 7.2210$	0.9357	0.9391	0.2001	0.59%
3	EGT	$Y_{EGT} = 0.6830\times + 226.4474$	0.9780	0.9255	5.1608	0.64%
4	Max Pressure	$Y_{pmax} = 0.8579\times + 10.9891$	0.8983	0.9946	2.2244	2.27%
5	Ignition delay	$Y_{ID} = 0.5352\times + 6.2391$	0.9601	0.9900	0.9459	5.87%
6	Smoke Emission	$Y_{smoke} = 0.6251\times + 23.0653$	0.9209	0.9888	1.4884	2.14%
7	CO	$Y_{CO} = 0.8239\times + 0.2212$	0.9384	0.9778	0.0804	5.88%
8	NO_x	$Y_{NO_x} = 0.4942\times + 6.8038$	0.9371	0.9591	0.5050	3.17%
9	HC	$Y_{HC} = 0.9036\times + 0.4977$	0.8521	0.9740	0.3661	4.85%

in NO_x emissions based on the investigation of the incorporation of Al_2O_3 nanoparticles can be ascribed to a confluence of interconnected elements. The Al_2O_3 nanoparticles serve to augment the thermal conductivity and catalytic possessions of fuel blends, possibly resulting in higher in-cylinder temperatures during the combustion stage. These increased temperatures are favourable to the generation of thermal-NO_xas described by the Zeldovich appliance. Moreover, Al_2O_3 may augment oxygen obtainability inside the combustion chamber, either by fostering improved atomization or promoting an additional complete burning procedure. The augmented presence of oxygen facilitates the formation of NO_x emissions. Furthermore, the duration of combustion may be influenced; specifically, if the incorporation of Al_2O_3 results in a higher could increase, thereby exacerbating NO_x emissions. Consequently, a comprehensive understanding of the observed trends in NO_x emissions necessitates consideration of the synergistic effects of higher in-cylinder temperatures, better oxygen availability, and modified

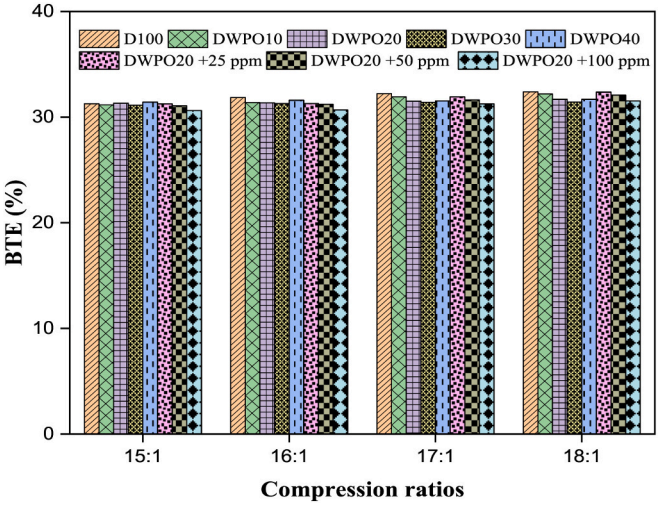

Fig. 9. BTE versus compression ratios.

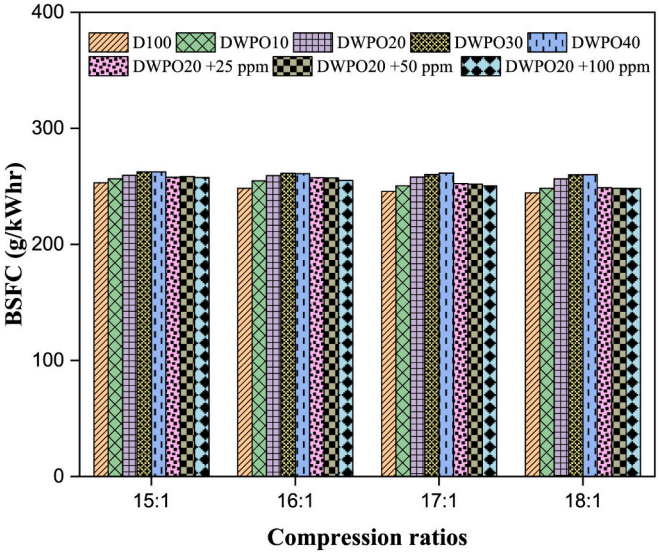

Fig. 10. BSFC versus compression ratios.

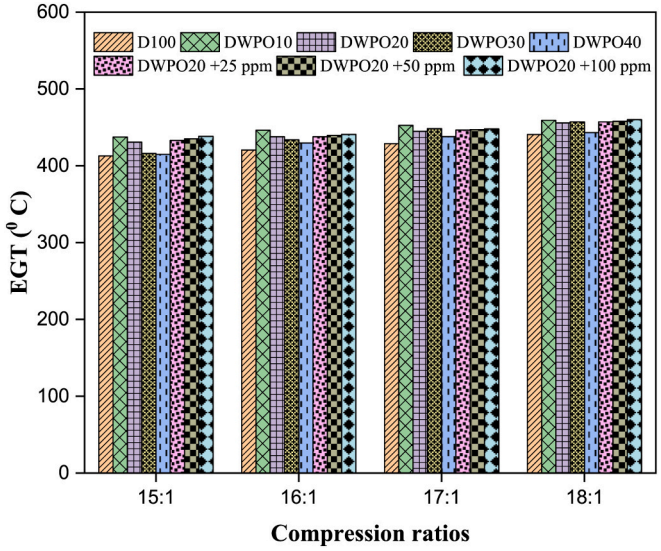

Fig. 11. EGT versus compression ratios.

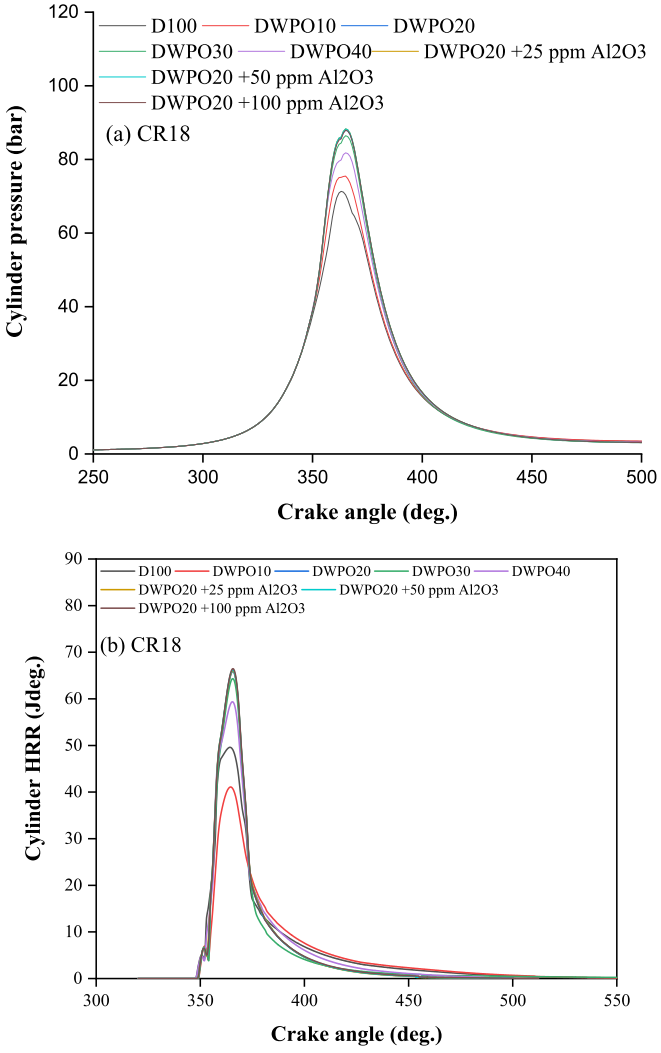

Fig. 12. a) P_{max} versus crank angle and b) HRR with CR18:1.

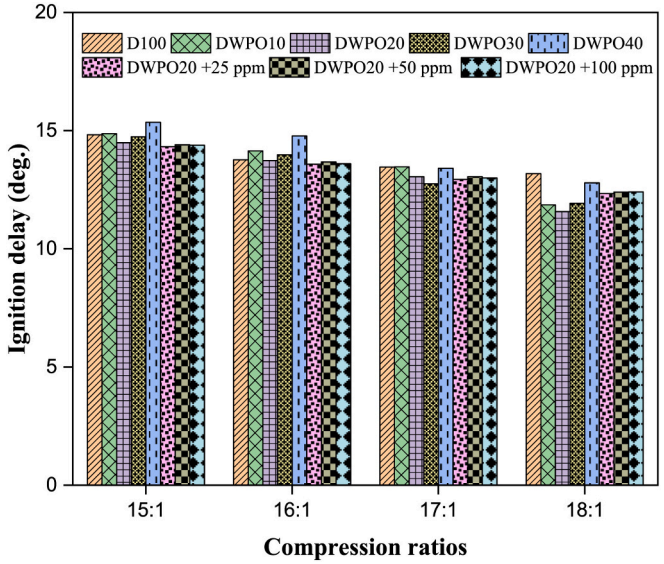

Fig. 13. ID versus engine compression ratios.

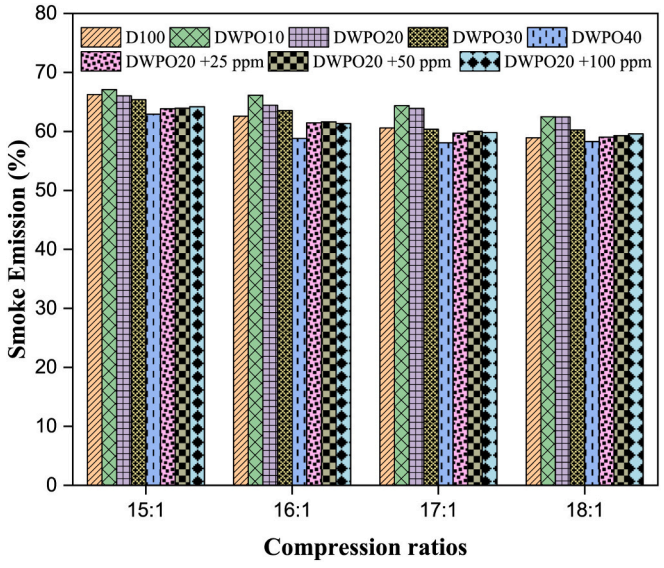

Fig. 14. Smoke emission versus compression ratios.

combustion duration [32–35]. The variation in NO_x emissions remains within expected uncertainty bounds and follows established thermal NO_x formation mechanisms, supporting the physical consistency of the results.

Fig. 17 shows the effect of WPO in diesel combined with Al_2O_3 nanoadditive on the engine NO_x emissions at full load conditions at CR15, CR16, CR17, and CR18 at 23°b TDC. Based on the findings, the DWPO10, DWPO20, DWPO30, and DWPO40 fuel blends have a slightly higher NO_x emission than that of D100. The NO_x emissions of DWPO10, DWPO20, DWPO30, and DWPO40 fuel blends at full load are 1.0%, 2.1%, 13.9%, and 13.9% higher at CR18, respectively, than those of the D100 fuel mix, respectively. In addition, compared to D100, the addition of nanoparticles (Al_2O_3) to the DWPO20 + 25 ppm, DWPO20 + 50 ppm, and DWPO20 + 100 ppm fuel blends leads to higher NO_x emissions during a full load of 15.2%, 16.05% and 15.25% at CR18:1.

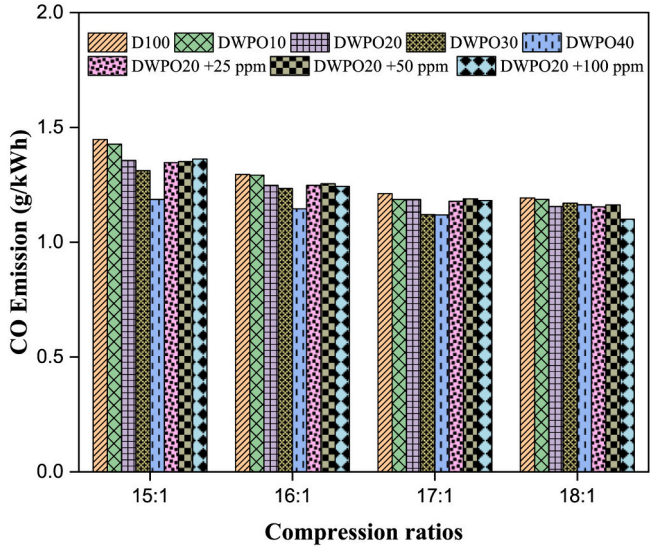

Fig. 15. CO emission versus compression ratios.

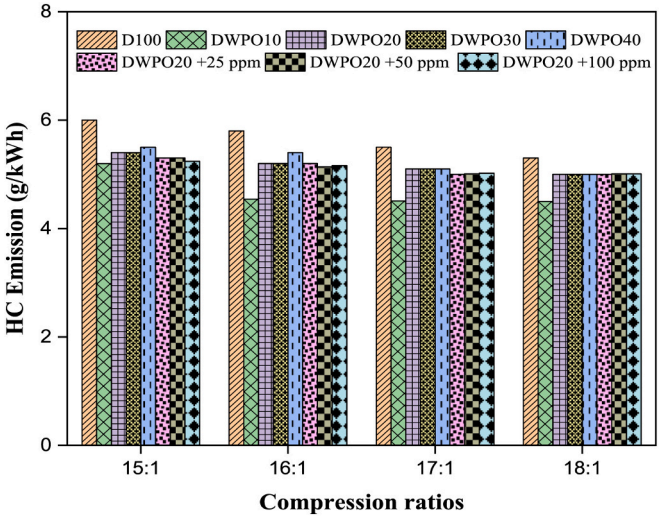

Fig. 16. HC emission versus compression ratios.

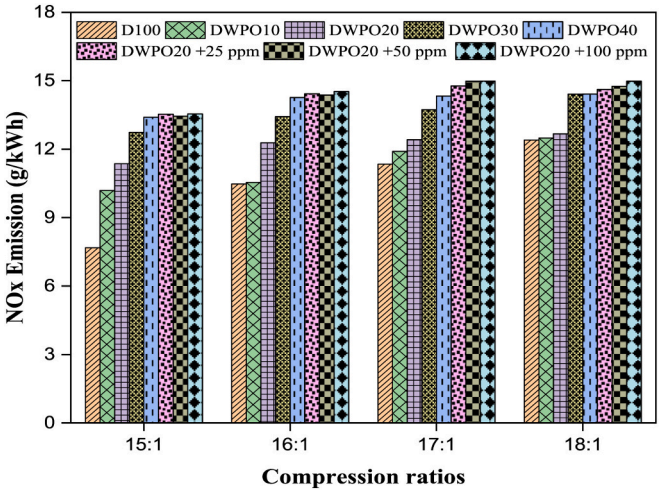

Fig. 17. NO_x emission versus compression ratios.

3.12. Performance-emission trade-off and practical applicability

The inclusion of Al_2O_3 nanoparticles does not lead to uniform enhancement under all of the working conditions and mixing ratios. Significant improvements in the BTE and reductions in CO and HC emissions can be seen mainly at the moderate blending ratios of WPO (up to 40%) and medium to high load rates, where the enhanced mixing of fuel and air and oxidation supported by nanoparticles are the most efficient. The higher the WPO fractions and the lower the low-load operation, the more the benefits diminish due to the rising viscosity of the fuel, lower calorific value, and incomplete combustion, limiting the catalytic and thermal impacts produced by nanoparticles. These results indicate that the influence of Al_2O_3 nanoparticles is strongly condition-dependent and governed by the combined effects of fuel properties, combustion temperature, and engine operating regime.

In favourable operating conditions, the performance of the engines with the addition of Al_2O_3 nanoparticles to the WPO-diesel blends could be observed to have improved significantly, indicated by increased BTE and less BSFC. Such advantages can be mainly credited to an increase in combustion efficiency, greater fuel atomization, and an increase in heat transfer in the combustion chamber. However, these efficiency gains were escorted by a rise in NO_x emissions, mainly at higher CRs, owing to increase in-cylinder temperatures and improved oxygen accessibility. Practically, the trade-off that was observed between the improvement in efficiency and NO_x the emission penalty is consistent with trends that were reported in the literature of nanoparticle-assisted combustion. Although the rise is NO_x is an environmental disadvantage, the scale of the penalty is not too large, and it can be potentially reduced by the means of the known control measures, including exhaust gas recirculation (EGR), optimization of the injection timing, after-treatment systems, or customized dosing of nanoparticles. Thus, the general findings reveal that Al_2O_3enhanced WPO-diesel mixtures can be taken as a potential way forward to enhance engine performance and fuel consumption, as long as the necessary measures of emission control are undertaken.

3.13. Comparison and validation of the research work

3.13.1. Comparison of ANN and GRNN

To compare the statistical similarity between experimental and estimated values through ANN and GRNN models, a paired sample *t*-test was done to show the level of statistical agreement as depicted in Fig. 18. The test R-values of the key performance and combustion parameters of BTE, BSFC, smoke opacity, and NO_x emissions, as well as ID, reveal good consistency between the predicted and experimental values (Tables 5 and 6). For instance, correlation coefficients of BTE with ANN and GRNN were 0.939 and 0.935, respectively, which showed that the prediction ability is statistically consistent. While both ANN and GRNN models exhibit high predictive accuracy, their performance varies slightly depending on the output parameter. ANN predictions showed marginally higher consistency for combustion-related parameters such as NO_x and ignition delay, whereas GRNN exhibited comparable or better accuracy for selected performance parameters. This difference is a manifestation of the difference in the structure of learning between iterative ANN training and memory-based GRNN regression. In general, the two models are strong predictors when assessed against experimental data.

Even though the ANN and the GRNN models were mainly tested concerning their predictive accuracy, they are also effective surrogate models used to analyse in an optimization-oriented manner. The models allow determining the desirable operating points between the enhancement of efficiency and emissions punishment by properly modelling the nonlinear relationships between CR, fuel blend composition, nanoparticle concentration, and engine responses. In the present study, ANN and GRNN predictions were employed to analyse parameter trends and trade-offs across the investigated operating space, thereby

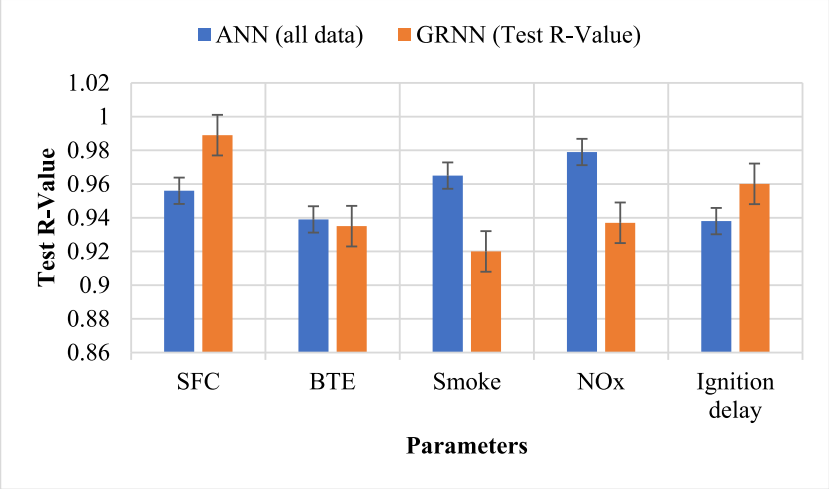

Fig. 18. Test R value for ANN and GRNN.

Table 8
Experimental and simulated data at CR18:1(D100).

Parameters	Experimental data	ANN predicted	GRNN Predicted
BTE (%)	33.2	32.888	32.983
BSFC (g/kWh)	244.3	245.427	248.501
EGT (K)	713.8	710.834	718.197
Max. CP (bar)	89.994	88.905	87.6877
Ignition delay (deg.)	13.58	13.486	13.477

providing model-assisted decision support for selecting optimal fuel engine combinations within the experimentally validated domain, rather than performing formal algorithm-based optimization.

3.13.2. Physical consistency of experimental and predicted results

In addition to statistical conformity, the AI models were evaluated in terms of the capacity to produce physically consistent tendencies in the experimental investigation. Predictions of both ANN and GRNN models are in close relation to the known behavior of CI engines concerning combustion and thermodynamics. A rise in CR led to an increase in BTE and peak cylinder pressure and a drop in ID, which is credited to an improvement in in-cylinder temperature and fuel-air mixing efficiencies. Both ANN and GRNN predictions were able to replicate the trends that were experimentally observed. Similarly, the progression NO_x with higher CRs, which is a well-known outcome of high combustion temperatures, was well reflected in the predicted outcome. The experimental and predicted results had minor deviations from each other, though these deviations were within reasonable limits of uncertainty and not contrary to physical laws. A specific instance of experimental and predicted data at a CR of 18:1 during diesel fuel operation is shown in Table 8, and it is observed that the figures are numerically close and exhibit similar trend behavior. It has been seen that the close correspondence between the predicted and known combustion mechanisms indicates that the AI models are physically informed predictive models and not merely statistical curve-fitting models. As a result, it can be concluded that the ANN and GRNN models have been confirmed in predictive analysis in the desired operating range and can be effectively applied to endorse the results of the experiment and parametric optimization.

4. Conclusions and future work

This study investigated the performance, combustion, and emission behavior of WPO-diesel blends that were augmented with Al_2O_3 nanoparticles in a single-cylinder/four-stroke/direct-injection/water-cooled Kirloskar TV1 CI engine operated at a constant speed (1500 rpm) and at different CRs of 15:1, 16:1, 17:1, and 18:1.

- The experiments were conducted under controlled laboratory conditions using a bowl-shaped piston to enhance air and fuel mixing. The outcomes indicate that an increase in CR positively affects BTE, while BSFC generally reduces with the rise in CR. Al_2O_3nanoparticles in WPO-diesel blends increased combustion efficiency, resulting in enhanced BTE and reduced BSFC in the blends as compared to similar blends without nanoparticles.
- These improvements are attributed to better atomization of the fuel, improved heat transfer, and the catalytic effects of the nanoparticles. The efficiency improvements were, however, accompanied by high levels of NO_x emission, especially at high CRs, owing to the high in-cylinder temperatures, high oxygen availability, and reduced duration of combustion. The DWPO20 blend with 25 ppm Al_2O_3 nanoparticles had the highest BTE, and the DWPO20 blend containing 100 ppm Al_2O_3 achieved the lowest BSFC at CR18.
- Combustion analysis indicated that the nanoparticle-enriched blends had high peak cylinder pressure, which appears to be in line with improved heat release characteristics. The developed ANN and GRNN models showed the high predictive power in the range of the investigation, which validates the dominant influence of load, CR, and fuel blend on engine performance and emissions.
- It is important to note that the outcomes of this work are based on laboratory-scale experiments carried out on a single-cylinder engine under steady-state conditions. While the findings indicate the potential of Al_2O_3 enhanced WPO-D100 blends to be used to enhance engine efficiency and fuel consumption, extreme care should be taken to extrapolate the findings to real-life or commercial applications.

The future work should thus be directed towards the long-term study of the durability to test the engine wear, lubricant degradation, and injector fouling, as well as the formation of deposits linked to the long-term use of nanoparticles. There is also a need to conduct research on the stability of nanoparticle dispersion in the long run and the effects it has on the parts of the fuel system. Further, scalability and robustness will have to be tested by validation over real-world engine operating conditions, such as multi-cylinder engines, variable speed and load operation, and transient driving cycles. The addition of emission reduction techniques like exhaust gas recirculation or after-treatment can further be used to supplement efficiency, reward, and punishment of NO_x emissions. Such initiatives will give a holistic evaluation of the viability and environmental sustainability of the utilization of nanoparticles in

assisting the use of WPO in CI engines.

Nomenclature

ANN	Artificial neural network
Al_2O_3	Aluminum oxide
BTE	Brake thermal efficiency
BSFC	Brake specific fuel consumption
GRNN	General regression neural network
WPO	Waste plastic oil
CR	Compression ratio
CI	Compression Ignition
HRR	Heat release rate
DE	Diesel engine
D100	100% diesel fuel
DWPO10	90% diesel fuel with 10% waste plastic oil
DWPO20	80% diesel fuel with 20% waste plastic oil
DWPO30	70% diesel fuel with 30% waste plastic oil
DWPO40	60% diesel fuel with 40% waste plastic oil
DWPO20 + 25 ppm	80% diesel fuel with 20% waste plastic oil and 25 ppm Al_2O_3
DWPO20 + 50 ppm	80% diesel fuel with 20% waste plastic oil and 50 ppm Al_2O_3
DWPO20 + 100 ppm	80% diesel fuel with 20% waste plastic oil and 100 ppm Al_2O_3
EGT	Exhaust gas temperature
ID	Ignition delay
HC	Hydrocarbon
CO	Carbon dioxide
NO_x	Nitrogen oxides

Generative AI and AI-assisted technologies

Not applicable.

CRediT authorship contribution statement

Upendra Rajak: Writing – review & editing, Writing – original draft, Validation, Methodology, Investigation, Conceptualization. **Manoj Panchal:** Supervision, Methodology, Data curation. **Abhishek Dasore:** Writing – review & editing, Formal analysis. **Norhashila Hashim:** Writing – review & editing, Supervision, Investigation. **Ramesh Chandra Mohanty:** Supervision, Formal analysis. **Nimay Chandra Giri:** Writing – review & editing, Formal analysis, Conceptualization. **Soumya Ranjan Das:** Resources, Funding acquisition.

Funding

The authors received no funding from an external source.

Declaration of competing interest

The authors declare no conflicts of interest.

Acknowledgments

The authors thank Manipal Academy of Higher Education, Manipal, India and RGM College of Engineering and Technology, Nandyal, India, for providing facilities to conduct the research.

Data availability

The data will be made available from the corresponding author upon reasonable request.

References

[1] C.Y. Zhang, et al., Which plastic recycling approaches maximize climate benefits and balance fossil energy? Evidence from the Japanese experience, Resour. Conserv. Recycl. 225 (2026) 108607, https://doi.org/10.1016/j.resconrec.2025.108607.
[2] P. Mishra, T. Mohapatra, S.S. Sahoo, B.N. Padhi, N.C. Giri, A. Emara, K.M. AboRas, Experimental assessment and optimization of the performance of a biodiesel engine using response surface methodology, Energy Sustain. Soc. 14 (2024) 28, https://doi.org/10.1186/s13705-024-00447-2.
[3] E. Gontarek-Castro, M. Haseler, M. Narra, A. Gołąbiewska, P.J. Trzebiatowska, Utilization routes of plastic waste from the marine environment: a review, Waste Manag. 210 (2026) 115221, https://doi.org/10.1016/j.wasman.2025.115221.
[4] T.S. Livingston, P. Madhu, C.S. Dhanalakshmi, R.V. Kumar, An experimental investigation on performance, emission and combustion characteristics of IC engine using liquid fuel produced through catalytic co-pyrolysis of pressed oil cake and mixed plastics with the addition of nanoparticles, Fuel 379 (2024) 133092, https://doi.org/10.1016/j.fuel.2024.133092.
[5] S. Li, J. Liu, F. Wang, Y. Li, M. Wei, H. Xiao, Z. An, Effects of gasoline and isobutanol addition on combustion and pollutant emissions of a common-rail diesel engine at different injection timing, Fuel 256 (2019) 115853, https://doi.org/10.1016/j.fuel.2019.115853.
[6] S.B. Arun, K.V. Yatish, G. Tigari, G.K. Prashanth, H.S. Lalithamba, K. Pramoda, Bio-based plant-extract facilitated MgO nanocatalyst for the transformation of agriculture waste derived-feedstock into biodiesel and as nano-additive in diesel engine, Renew. Energy 256 (Part D) (2026) 124218, https://doi.org/10.1016/j.renene.2025.124218.
[7] T. Anand, S. Debbarma, Experimental investigation of fuel injection timing effects on a CRDI diesel engine running on hydrogen-enriched waste plastic oil, Int. J. Hydrogen Energy 57 (2024) 1051–1069, https://doi.org/10.1016/j.ijhydene.2024.01.052.
[8] J.G. John, V. Hariram, V.S.S. Kavuru Rakesh, T. Harsha-Vardhan, T.Y. Vamsi-Manikanta, S. Shafi, Waste cooking oil biodiesel with FeO nanoparticle – a viable alternative fuel source, Mater. Today 72 (2023) 1991–1995, https://doi.org/10.1016/j.matpr.2022.07.289.
[9] B.H. Tambunan, H. Ambarita, T.B. Sitorus, A.H. Sebayang, Experimental study of the use of plastic pyrolysis oil as an additive to improve physicochemical properties and performance rubber seed biodiesel, Case Stud. Chem. Environ. Eng. 10 (2024) 100924, https://doi.org/10.1016/j.cscee.2024.100924.
[10] P. Murugesan, P.V. Elumalai, D. Balasubramanian, S. Padmanabhan, N. Murugunachippan, A. Afzal, P. Sharma, K. Kiran, J.F. Josephin, E.G. Varuvel, T. T. Le, Exploration of low heat rejection engine characteristics powered with carbon nanotubes-added waste plastic pyrolysis oil, Process Saf. Environ. Prot. 176 (2023) 1101–1119, https://doi.org/10.1016/j.psep.2023.06.051.
[11] S.P. Sundar, P. Vijayabalan, R. Sathyamurthy, Z. Said, A.K. Thakur, Experimental and feasibility study on nano blended waste plastic oil-based diesel engine at various injection pressure: a value addition for disposed plastic food containers, Fuel Process. Technol. 242 (2023) 107627, https://doi.org/10.1016/j.fuproc.2022.107627.
[12] P. Sankar, M. Thangavelu, V. Moorthy, S.M. Subhani, R. Manimaran, Prediction and optimization of diesel engine characteristics for various fuel injection timing: operated by third generation green fuel with alumina nano additive, Sustain. Energy Technol. Assess. 53 (2022) 102751, https://doi.org/10.1016/j.seta.2022.102751.
[13] S. Mehanathan, P. Madhu, C.S. Dhanalakshmi, R. Vijayakumar, Synergistic recovery of renewable hydrocarbon resources via co-pyrolysis of non-edible linseed and waste polypropylene: a study on influence of plastic on oil production and their utilization as a fuel for IC engine, J. Energy Inst. 118 (2025) 101905, https://doi.org/10.1016/j.joei.2024.101905.
[14] G. Ionescu, R.N. State, M. Pătraşcu, A. Volceanov, C. Gheorghe, D. Boldor, C. Mărculescu, Production of co-formulants for biodiesel from waste mixtures pyrolysis oil through Fe-based catalysts, Biomass Bioenergy 182 (2024) 107088, https://doi.org/10.1016/j.biombioe.2024.107088.
[15] D. Damodharan, B. Rajesh Kumar, K. Gopal, M.V. De Poures, B. Sethuramasamyraja, Utilization of waste plastic oil in diesel engines: a review, Rev. Environ. Sci. Biotechnol. 18 (4) (2019) 681–697, https://doi.org/10.1007/s11157-019-09516-x.
[16] M. Rycroft, Waste plastic to fuel oil: an under-exploited opportunity for energy generation. Process. Saf. Environ. Prot.112 (2017) 3–10. doi:https://doi.org/10.1016/j.joei.2022.101154.
[17] E. Butler, G. Devlin, K. McDonnell, Waste polyolefins to liquid fuels via pyrolysis: review of commercial state-of-the-art and recent laboratory research, Waste Biomass Valoriz. 2 (3) (2011) 227–255, https://doi.org/10.1007/s12649-011-9067-5.
[18] G. Kavitha, A. Manikandan, G.M. Raja, R.L. Krupakaran, D. Balasubramanian, V. Q. Nguyen, A.T. Hoang, J.F. Josephin, S.A. Alharbi, E.G. Varuvel, Thermodynamic and emission analysis of waste plastic oil fuelled diesel engine with Ce-Al catalyst-based catalytic converters–an experimental study, Process Saf. Environ. Protect. 197 (2025) 106997, https://doi.org/10.1016/j.psep.2025.106997.
[19] H. Yaqoob, H.M. Ali, U. Sajjad, K. Hamid, Investigating the potential of plastic pyrolysis oil-diesel blends in diesel engine: performance, emissions, thermodynamics and sustainability analysis, Results Eng. 24 (2024) 103336, https://doi.org/10.1016/j.rineng.2024.103336.
[20] K.S. Kumar, S. Muniamuthu, T.Y. Khan, A. Razak, Performance evaluation of a diesel engine fuelled with waste plastic pyrolysis oil, 1-butanol, and CeO2 additives

under varying injection pressures, Case Stud. Therm. Eng. 72 (2025), https://doi.org/10.1016/j.csite.2025.106284.
[21] A. Afzal, R.G. Roy, C.P. Koshy, M. Abbas, E. Cuce, R.K. Rajak, S. Shaik, C.A. Saleel, Characterization of biodiesel based on plastic pyrolysis oil (PPO) and coconut oil: Performance and emission analysis using RSM-ANN approach, Sustain Energy Technol Assess 56 (2023) 103046, https://doi.org/10.1016/j.seta.2023.103046.
[22] D. Kundu, A. Barathi, K. Pooja, M. Surya, S. Jacob, P. Samanta, V. Kumar, H. Singh, M.D. Adhikari, Aligning policy, sustainability metrics and environmental assessment for biofuels: a comprehensive review, Bioresour. Technol. Rep. 32 (2025) 102300, https://doi.org/10.1016/j.biteb.2025.102300.
[23] S. Razmi, H. Mirzaee, G. Kumar, T. Sowlati, Applications of machine learning for decision support in biomass supply chains: a systematic review, Comput. Chem. Eng. 205 (2026) 109451, https://doi.org/10.1016/j.compchemeng.2025.109451.
[24] K.K. Januszewicz, J. Hunicz, P. Kazimierski, A. Raybak, T. Suchocki, K. Duda, M. Mikulski, An experimental assessment on a diesel engine powered by blends of waste-plastic-derived pyrolysis oil with diesel, Energy 281 (2023) 128330, https://doi.org/10.1016/j.energy.2023.128330.
[25] S. Deng, L. Wang, S. Kim, B.C. Koenig, Scientific machine learning in combustion for discovery, simulation, and control, Proc. Combust. Inst. 41 (2025) 105796, https://doi.org/10.1016/j.proci.2025.105796.
[26] M.S. Abishek, S. Kachhap, U. Rajak, T.N. Verma, N.C. Giri, K.M. AboRas, A. ELrashidi, Exergy-energy, sustainability, and emissions assessment of *Guizotia abyssinica* (L.) fuel blends with metallic nano additives, Sci. Rep. 14 (1) (2024) 3537, https://doi.org/10.1038/s41598-024-53963-8.
[27] P. Aengchuan, A. Wiangkham, N. Klinkaew, K. Theinnoi, E. Sukjit, Prediction of the influence of castor oil–ethanol–diesel blends on single-cylinder diesel engine characteristics using generalized regression neural networks (GRNNs), Energy Rep. 8 (2022) 38–47, https://doi.org/10.1016/j.egyr.2022.10.113.
[28] H. Kuszewski, Experimental investigation of the autoignition properties of ethanol–biodiesel fuel blends, Fuel 235 (2019) 1301–1308, https://doi.org/10.1016/j.fuel.2018.08.146.
[29] C. Satapathy, S.K. Nayak, P.C. Mishra, N. Kaliappan, K.K. Priya, Assessment of engine characteristics in dual-fuel mode using post-mixed biodiesel and coconut shell producer gas, Results Eng. 27 (2025) 106976, https://doi.org/10.1016/j.rineng.2025.106976.
[30] A.I. EL-Seesy, R.M. El-Zoheiry, M.I. Hassan Ali, Enhancing jojoba biodiesel performance in diesel engines using diethyl ether and functionalized multiwalled carbon nanotubes, Fuel Process. Technol. 277 (2025) 108304, https://doi.org/10.1016/j.fuproc.2025.108304.
[31] J. Hunicz, A. Rybak, D. Szpica, M.S. Gęca, P. Woś, L. Yang, M. Mikulski, Waste plastic pyrolysis oils as diesel fuel blending components: detailed analysis of combustion and emissions sensitivity to engine control parameters, Energy 313 (2024) 134093, https://doi.org/10.1016/j.energy.2024.134093.
[32] N.C. Belay, B.A. Fentaw, R.B. Nallamothu, M.S. Kebede, Performance evaluation of liquid fuel derived from waste plastics for diesel engine applications and emissions characteristics, Energy 318 (2025) 134911, https://doi.org/10.1016/j.energy.2025.134911.
[33] I. Kalargaris, G. Tian, S. Gu, Experimental evaluation of a diesel engine fuelled by pyrolysis oils produced from low-density polyethylene and ethylene–vinyl acetate plastics, Fuel Process. Technol. 161 (2017) 125–131, https://doi.org/10.1016/j.fuproc.2017.03.014.
[34] M. Karagöz, F. Polat, S. Sarıdemir, M.K. Yeşilyurt, Ü. Ağbulut, An experimental assessment on dual fuel engine behavior powered by waste tire-derived pyrolysis oil – biogas blends, Fuel Process. Technol. 229 (2022) 107177, https://doi.org/10.1016/j.fuproc.2022.107177.
[35] K. Yeneneh, G. Sufe, Enhancing diesel engine performance and emissions using alumina nanoparticle-blended waste plastic oil biodiesel: an experimental and predictive approach, Ind. Eng. Chem. Res. 64 (24) (2025) 11681–11694, https://doi.org/10.1021/acs.iecr.5c01296.